Unraveling the genetics of polyamine metabolism in barley for senescence-related crop improvement

Umesh Kumar Tanwar
Department of Plant Physiology, Faculty of Biology, Adam Mickiewicz University, ul. Uniwersytet Poznańskiego 6, 61-614 Poznań
Ewelina Stolarska
Department of Plant Physiology, Faculty of Biology, Adam Mickiewicz University, ul. Uniwersytet Poznańskiego 6, 61-614 Poznań
Ewelina Paluch-Lubawa
Department of Plant Physiology, Faculty of Biology, Adam Mickiewicz University, ul. Uniwersytet Poznańskiego 6, 61-614 Poznań
Autar K. Mattoo
Sustainable Agricultural Systems Laboratory, United States Department of Agriculture, Agricultural Research Service, Henry A. Wallace Beltsville Agricultural Research Center, Beltsville, MD 20705-2350
Magdalena Arasimowicz-Jelonek
Department of Plant Ecophysiology, Faculty of Biology, Adam Mickiewicz University, ul. Uniwersytet Poznańskiego 6, 61-614 Poznań
Ewa Sobieszczuk-Nowicka (ewa.sobieszczuk-nowicka@amu.edu.pl)
Department of Plant Physiology, Faculty of Biology, Adam Mickiewicz University, ul. Uniwersytet Poznańskiego 6, 61-614 Poznań

Article

Keywords: Model crop plant, Abiotic stress, Gene expression, Genome-wide identification, Gramineae, Hordeum vulgare, Leaf senescence, Polyamine metabolic pathway

Posted Date: May 26th, 2022

DOI: https://doi.org/10.21203/rs.3.rs-1665637/v1

Abstract

We explored the polyamine (PA) metabolic pathway genes in barley (Hv) to understand plant development and stress adaptation in *Gramineae* crops with emphasis on leaf senescence.

Bioinformatics and functional genomics tools were utilized for genome-wide identification, comprehensive gene features, evolution, development and stress effects on the expression of the polyamine metabolic pathway gene families (PMGs). Three S-adenosylmethionine decarboxylases (*HvSAMDCs*), two ornithine decarboxylase, one arginine decarboxylase, one spermidine synthase (*HvSPDS*), two spermine synthases (*HvSPMSs*), five copper amine oxidases (*HvCuAO*) and seven polyamine oxidases (*HvPAOs*) members of PMGs were identified and characterized in barley. All the genes except for *HvCuAO3* were found distributed on all chromosomes of barley. The phylogenetic and comparative assessment revealed that PA metabolic pathway is highly conserved in plants and the prediction of nine *H. vulgare* miRNAs (hvu-miR) target sites, 18 protein-protein interactions and 961 putative CREs in the promoter region were discerned. Gene expression of *HvSAMDC3*, *HvCuAO7*, *HvPAO4* and *HvSPMS1* were apparent at every developmental stage. *SPDS/SPMS* gene family was found to be the most responsive to induced leaf senescence.

This study provides a reference for the functional investigation of the molecular mechanism(s) that regulate polyamine in plants as a tool for future breeding decision management systems.

Introduction

Barley (*Hordeum vulgare*), a member of the grass family, is one of the major and important crops as it ranks fourth among grain cereals (Gramineae species) after maize, wheat, and rice in terms of global production[1]. The global production volume of barley was estimated as 159.74 million metric tons in the 2020/2021 crop year (https://www.statista.com/statistics/271973/world-barley-production-since-2008/). Barley is self-pollinating with a diploid genome consisting of seven chromosomes (2n = 2x = 14). The estimated genome size of barley is 5.1 Gbp, with > 80% of repetitive elements[2]. Although it has a large genome, barley is considered as a good genomic model for cultivated hexaploid wheat due to its simple diploid genome. In particular, many barley and wheat genes have similar functions. Therefore, information about a gene in barley can therefore be readily applicable to estimate the genes responsible for similar traits in wheat[1]. This makes barley unique among crop plants as it is tremendously important for agriculture and for science. Advances on both fronts create a positive feedback loop, allowing barley to be in the forefront in meeting the great challenges of climate change and human population growth[3].

Crop losses due to climate change and different abiotic stressors adversely affect agriculture and crop production, factors that impact sustainability of food production. Extreme temperatures (cold, freezing or heat), drought, and salinity are some of the known major stressors[4–12]. Each of these stressors imposes specific complexity in biological and genetic response of a plant and therefore to solutions to mitigate them. Thus, it is important to develop a good understanding of the complex response(s) inherent to each abiotic stress and catalog/delineate them for each crop plant to enable translational research. A number of reviews have focused on several aspects of plant abiotic stresses and highlighted the important need for delineating the processes involved and possible ways to mitigate them by utilizing 'antistress effectors', developing new genetic approaches, and creating new resilient crops[4,8,10–13]. To improve crop management, enhance yield, and quality of barley, it is important to elucidate the molecular mechanistic details of development and stress resistance.

Polyamines (PAs) are low molecular weight aliphatic nitrogenous bases containing two or more amino groups, which are found in different life forms ranging from prokaryotes to eukaryotes[14–16]. Increasing evidence supports the importance of PAs in all domains of life[17,18]. Polyamines are essential for cellular viability through their role(s) in critical cellular functions, including regulation of nucleic acids and protein synthesis, and macromolecular structural integrity[19,20]. Many of the regulatory mechanisms of PAs are broadly conserved in cells, which is suggestive of their regulation to be of great importance[21,22]. PAs homeostasis is tightly regulated, with excessive intracellular PAs in certain tissues leading to undesired[23] and desired phenotypes[19,24]. In plants, putrescine (Put), spermidine (Spd) and spermine (Spm) are the major PAs, and they are involved in the regulation of diverse physiological processes, such as flower development, embryogenesis, organogenesis, senescence, fruit maturation and development, and in responses to biotic and abiotic stresses. Molecular biotechnology techniques have provided increasing evidence that PAs, whether applied exogenously or produced endogenously via genetic engineering, can positively affect plant growth, productivity, and stress tolerance[17]. Correlations between plant production parameters (e.g., grain filling rate and yield components) and PA contents have also been reported[21,25]. Manipulation of polyamine metabolism may also result in improved assimilation of N and C in plants, and consequently improving plant nitrogen use efficiency and reducing the use of fertilizers[26].

Recent advances in genomics have made it possible to develop large-scale sequence data for many crop species[27]. Such datasets have been useful for understanding the genome architecture/dynamics and have facilitated the gene discovery. A major challenge is to translate genome information to develop superior lines for trait(s) of interest [28]. The enormous resource of completely decoded genomes of diverse species has made it possible to better understand their evolution at the molecular level, identifying gene functions, decoding pathways, and elucidating complex genetic regulation. Databases and tools have consistently organized the genomic data according to phylogenetic, functional, and structural principles, which have led to increased resolution power and robustness of the analysis of diverse genomes. Multiple genomic resources have been developed to analyze partial or total genomic sequences and their associated functions in barley[1,29–32]. However, studies of genome-wide genetic diversity in barley have so far mainly focused on single nucleotide polymorphisms (SNPs) and short insertions and deletions (indels) in genic regions[1].

Polyamine metabolism genes have been identified in several plant species[20,33–40], while little systematic genome-wide PA metabolic pathway genes (PMGs) studies have been conducted. Further functional characterization of PMGs, which constitute a large family of enzymes in plant metabolism, is little known in the Gramineae crops. Most of the barley genes of PA metabolism except for SPMS and PAOs have yet to be identified and characterized[41,42]. We present here the first genome-wide identification, isolation, comprehensive gene features, evolution, expression analysis of the PA metabolic pathway gene families, and

analysis on their physiochemical characteristics, as well as the role of PMGs in development and stress adaption, in barley, with particular emphasis to leaf senescence. Senescence occurs in an organized process to dismantle the vegetative tissues and redirect nutrients towards metabolic pathways for reproductive success[43]. Economic impact of senescence is of great interest since it effect grain and yield quality[44]. Importantly, the direction of PA metabolism, anabolism vs catabolism plays a central role in metabolic reprogramming and determining when a senescing leaf enters programmed organ death.

Results

1. Identification of polyamine metabolic pathway genes in barley and physiochemical characterization of proteins

Protein homology search was carried out with known PA metabolic pathway proteins from Arabidopsis and rice to search for the PMG proteins in barley, *Hordeum vulgare* cv. Golden Promise, using a Hidden Morkov Model (HMM). Based on BLASTP search, a total of 23 PA metabolic pathway genes in barley were identified (Table 1). These genes include one arginine decarboxylase (*HvADC1*), two ornithine decarboxylases (*HvODC1* and *HvODC2*), three S-adenosylmethionine decarboxylases (*HvSAMDC1*-3), nine polyamine oxidases (*HvPAO1*-9), and five diamine/copper-containing amine oxidases (*HvCuAO2*, 3, 4, 6, and − 7). Three other genes identified are one spermidine synthase (*HvSPDS1*) and two spermine synthases (*SPMS1* and *SPMS2*). Notably, in this search, no thermospermine synthase-like (*tSPMS*/*ACULIS5*-like) gene was found in the *H. vulgare* genome. The identified gene sequences were then amplified by PCR (Supplementary Fig. S1) and confirmed by sequencing.

Table 1
Physiochemical characteristics of 23 barley polyamine metabolic pathway proteins identified in current study. *ADC* (arginine decarboxylase); *SAMDC* (S-ader decarboxylase); *SPDS* (spermidine synthase); *SPMS* (spermine synthase); CuAO (Diamine or copper-containing oxidase); and *PAO* (polyamine oxidase) in

Gene name	Gene ID	Transcript ID	Strand	CDS (bp)	Protien (aa)	Molecular weight (Da)	pI	GRAVY	Subcellular localization	N-termir transit/s peptide
HvSAMDC1	HORVU5Hr1G064040	HORVU5Hr1G064040.8	Forward	1329	442	47420.83	5.04	-0.039	Chloroplast, Nucleus	Other
HvSAMDC2	HORVU6Hr1G056110	HORVU6Hr1G056110.3	Reverse	1421	389	42307.89	4.92	-0.123	Cell membrane, Chloroplast, Nucleus	Other
HvSAMDC3	HORVU2Hr1G086140	HORVU2Hr1G086140.5	Reverse	1353	450	48910.58	5.18	-0.101	Chloroplast	Other
HvPAO1	HORVU4Hr1G071450	HORVU4Hr1G071450.1	Forward	1988	568	63733.49	7.74	-0.281	Chloroplast	Thylako luminal transfer peptide
HvPAO2	HORVU7Hr1G090410	HORVU7Hr1G090410.1	Reverse	1912	503	56524.04	6.19	-0.331	Chloroplast	Signal peptide
HvPAO3	HORVU7Hr1G118260	HORVU7Hr1G118260.1	Forward	1688	498	55803.36	5.99	-0.277	Chloroplast	Signal peptide
HvPAO4	HORVU2Hr1G103220	HORVU2Hr1G103220.3	Reverse	2389	484	53661.17	5.29	-0.058	Chloroplast	Other
HvPAO5	HORVU3Hr1G066920	HORVU3Hr1G066920.1	Forward	3535	510	54999.32	5.4	-0.157	Chloroplast	Other
HvPAO6	HORVU7Hr1G118240	HORVU7Hr1G118240.1	Forward	1823	495	55484.15	6.54	-0.298	Chloroplast	Signal peptide
HvPAO7	HORVU2Hr1G121060	HORVU2Hr1G121060.1	Forward	2327	489	53222.94	5.47	-0.04	Chloroplast	Other
HvPAO8	HORVU2Hr1G121050	HORVU2Hr1G121050.1	Forward	2258	492	54318.22	5.36	-0.005	Chloroplast	Other
HvPAO9	HORVU6Hr1G091060	HORVU6Hr1G091060.1	Reverse	1496	435	49972.46	5.75	-0.445	Chloroplast	Other
HvSPMS1	HORVU5Hr1G052890	HORVU5Hr1G052890.2	Reverse	1692	385	42010.05	5.53	-0.15	Cytoplasm	Other
HvSPMS2	HORVU7Hr1G079430	HORVU7Hr1G079430.2	Reverse	5130	440	49016.63	8.64	-0.166	Chloroplast	Other
HvSPDS1	HORVU7Hr1G055560	HORVU7Hr1G055560.1	Forward	1696	263	28713.64	4.94	-0.038	Cytoplasm	Other
HvCuAO2	HORVU4Hr1G074530	HORVU4Hr1G074530.5	Forward	2112	703	na	na	-0.137	Peroxisome	Signal peptide
HvCuAO3	HORVU0Hr1G009050	HORVU0Hr1G009050.1	Reverse	558	186	na	na	-0.102	Cell wall	Other
HvCuAO4	HORVU2Hr1G012710	HORVU2Hr1G012710.2	Reverse	1879	560	62041.66	9.41	-0.461	Chloroplast	Other
HvCuAO6	HORVU6Hr1G053060	HORVU6Hr1G053060.9	Reverse	2133	677	76755.41	6.46	-0.384	Peroxisome	Other
HvCuAO7	HORVU2Hr1G082420	HORVU2Hr1G082420.5	Reverse	1760	585	66378.31	6.23	-0.43	Cell wall, Peroxisome	Other
HvADC1	HORVU1Hr1G002090	HORVU1Hr1G002090.11	Forward	2022	614	67032.73	6.13	-0.139	Chloroplast, Cytoplasm, Mitochondrion	Other
HvODC1	HORVU5Hr1G084750	HORVU5Hr1G084750.1	Forward	1756	408	43608.78	5.46	0.013	Chloroplast	Other
HvODC2	HORVU7Hr1G032100	HORVU7Hr1G032100.1	Forward	721	208	na	na	-0.201	Chloroplast	Other

The physiochemical characteristics of the identified PA metabolic pathway proteins in barley are presented in Table 1. The CDS sequence of *Hv*PMG genes ranged from 558 bp (*HvCuAO3*) to 3535 bp (*HvPAO5*), while the length of protein sequences ranged from 186 (HvCuAO3) to 703 (HvCuAO2) amino acids. The average molecular weight size was 53.60 kDa, varying between 28.71 kDa (HvSPDS3) and 76.75 kDa (HvCuAO6). The HvPMG proteins had relatively low isoelectric point (pI < 7), with pI of 7.74, 8.64 and 9.41, respectively, for HvPAO1, HvSPDS2 and HvCuAO4. All the proteins had negative GRAVY values in the range of -0.005 (HvPAO8) to -0.461 (HvDAO4), except for HvODC1 which was GRAVY 0.013. Sub-cellular localization prediction showed that 18 out of 23 HvPMG proteins localized to chloroplast, while the remaining ones localized to cytoplasm, peroxisome and cell wall. Multiple localization was predicted for HvSAMDC1 (chloroplast, nucleus), HvSAMDC2 (cell membrane, chloroplast, nucleus), HvCuAO7 (cell wall, peroxisome) and HvADC1 (chloroplast, cytoplasm, mitochondrion). Analysis for N-terminal transit/signal peptide prediction detected only two signal peptides in HvPMG proteins - thylakoid luminal transfer peptide (HvPAO1) and Signal peptide (HvPAO2, HvPAO3, HvPAO6, HvCuAO2). Most of the HvPMG proteins did not harbour any trans-membrane domains, except for HvPAO3, HvPAO3 and HvCuAO2 which had one trans-membrane helix.

2. Gene structure, protein sequence alignment and phylogenetic analysis

Gene structure, exon and intron information was obtained for the identified 23 *Hv*PMG genes to interrogate their genomic organization (Fig. 1A). The *Hv*PMG genes were clustered closely as per the phylogenetic analysis and subfamily classification mentioned above. Intron-exon organization of the *Hv*PMGs indicated that *HvODC1-2, HvPAO5, HvSPDS1* and *HvSAMDC2* genes were intron-less, while all other genes contained a varying number of introns ranging from 1 to 11. *HvCuAOs* were diverse in gene structure, containing 3 (*HvCuAO3*) to 11 (*HvCuAO6*) exons separated by 2 to 10 intergenic regions. Similar structure was found for *HvSAMDC* genes which contained 1 (*HvSAMDC2*) to 2 (*HvSAMDC1*and 3) exons, and all the three genes shared 1 large exon. *HvSPDS1* gene was intron-less containing only one large exon, while *HvSPMS1*and 2 had distantly located 11 and 12 small exons, respectively. *HvPAO* genes were more diverse in their genomic organization containing 1 (*HvPAO5*) to 10 (*HvPAO8*) exons while *HvADC1* has 3 exons, and both *HvODCs* contain 1 exon.

Next, we analysed the identified HvPMG protein sequences using Hidden Markov Model (HMM) analysis for the presence of a typical HMM signature domain representing the corresponding protein class in a HMMER search (Table 2). Domain analysis revealed that HvSAMDCs possesses PF01536 (adenosylmethionine decarboxylase) and PF08132 (S-adenosyl-l-methionine decarboxylase leader peptide) similar to the land plant SAMDc proteins. Three SPDS/SPMS-like proteins, HvSPMS1 and 2, and HvSPDS1, contained the signature HMM profiles common for spermine/spermidine synthase domain (PF01564) and spermidine synthase tetramerization domain (PF17284) similar to SPDS/SPMS proteins of Arabidopsis and rice. The domain PF02784 (pyridoxal-dependent decarboxylase, pyridoxal binding domain) was found on HvADC and HvODCs, with ODCs possessing additional pyridoxal-dependent decarboxylase, C-terminal sheet domain (PF00278). All the polyamine oxidases (HvPAOs 1–9) contained only one domain PF01593 (flavin containing amine oxidoreductase), while the copper-containing amine oxidases (HvCuAOs) contained multiple domains, namely, PF01179 (copper amine oxidase, enzyme domain), PF02728 (copper amine oxidase, N3 domain), and PF02727 (copper amine oxidase, N2 domain).

Table 2
Location of signature domains in barley polyamine metabolic pathway protein sequences. *ADC* (arginine decarboxylase); *SAMDC* (S-adenosylmethionine decarboxylase); *SPDS* (spermidine synthase); *SPMS* (spermine synthase); CuAO (Diamine or copper-containing oxidase); and *PAO* (polyamine oxidase) in barley (*Hv*).

Name	Size (aa)	Hidden Markov model domains (N→C)
HvSAMDC1	442	PF01536 (66–393),PF08132 (1–44)
HvSAMDC2	389	PF01536 (7-333)
HvSAMDC3	450	PF01536 (66–392),PF08132 (1–49)
HvPAO1	568	PF01593 (110–550)
HvPAO2	503	PF01593 (38–477)
HvPAO3	498	PF01593 (38–480)
HvPAO4	484	PF01593 (28–447)
HvPAO5	510	PF01593 (15–506)
HvPAO6	495	PF01593 (35–477)
HvPAO7	489	PF01593 (33–453)
HvPAO8	492	PF01593 (35–454)
HvPAO9	435	PF01593 (2-418)
HvSPMS1	385	PF17284(72–120), PF01564 (124–308)
HvSPMS2	440	PF17284(129–175), PF01564 (179–363)
HvSPDS1	263	PF17284(35–89), PF01564 (92–261)
HvCuAO2	703	PF01179 (269–680), PF02728 (144–242), PF02727 (44–127)
HvCuAO3	183	PF01179 (1-178)
HvCuAO4	560	PF01179 (72–403), PF02728 (3–40)
HvCuAO6	677	PF01179 (264–670), PF02728 (133–237), PF02727 (8–92)
HvCuAO7	585	PF01179 (148–554), PF02728 (21–121)
HvADC1	614	PF02784 (110–369)
HvODC1	408	PF00278 (52–382), PF02784 (57–289)
HvODC2	208	PF00278 (85–182), PF02784 (27–84)

PF01536: Adenosylmethionine decarboxylase; PF08132: S-adenosyl-l-methionine decarboxylase leader peptide; PF01593: Flavin containing amine oxidoreductase; PF17284: Spermidine synthase tetramerisation domain; PF01564: Spermine/spermidine synthase domain; PF01179: Copper amine oxidase, enzyme domain; PF02728: Copper amine oxidase, N3 domain; PF02727: Copper amine oxidase, N2 domain; PF02784: Pyridoxal-dependent decarboxylase, pyridoxal binding domain; PF00278: Pyridoxal-dependent decarboxylase, C-terminal sheet domain

Phylogenetic tree analysis of the identified barley genes, *Hv*PMGs, was compared to that of Arabidopsis, rice and maize plants. It revealed that PA metabolic pathway proteins are highly conserved in these four species, with SAMDCs, PAOs, CuAOs, ADCs, ODCs, and SPDS/SPMSs being clustered into one group each, respectively (Fig. 1B). We further compared the PA metabolic genes structures and protein sequences of barley with Arabidopsis, rice and maize plants

(Fig. 2A-J). In case of the SAMDC sequences, three barley genes clustered in different branches. Several SAMDC genes (except for *OsSAMDC5* and *OsSAMDC6*) were highly similar in their protein motifs, differing only slightly in gene structure (Fig. 2A and 2B). Comparison with amino oxidases revealed that eight *HvPAOs* and five *CuAOs* genes distributed in different clusters of similar protein motifs along with the other plant oxidases and varied in gene structure with having 0–8 introns (Fig. 2C-F). *HvADC1* has two introns while other plant *ADCs* are intronless (Fig. 2G). Despite this all the *ADCs* were clustered in one group and shared a highly conserved protein motif sequence (Fig. 2H). The six *ODCs* in barley, rice, and maize clustered into different groups, but had highly similar protein motif constructions, and none of these genes had more than one intron (Fig. 2G and 2H). For *SPMS*/ *SPDS* analysis, fifteen genes from our comparative species clustered into three groups based on the presence of similar protein motifs. Examination of the structure revealed that all these genes, except for *HvSPDS1*, contained multiple introns in their sequences, while possessing highly similar protein motif constructions (Fig. 2I and 2J). The sequence details of each motif (1–10) and construction of protein sequences displayed in different coloured boxes in Fig. 2 are provided in the Supplementary Tables S2-6 and Supplementary Fig. S2-6. In addition, multiple protein sequence alignments of barley genes with that of Arabidopsis, rice and maize were also carried out to show the conserved catalytic residues (Supplementary Fig. S7-11).

3. Chromosomal location, gene duplication and evolutionary rate calculations

Based on the physical location information from the database of barley genome, the chromosomal location of *Hv*PMG genes was determined (Supplementary Fig. S12). All the identified *Hv*PMG genes were distributed on all seven chromosomes except for *HvCuAO3* which was located on ChrUn (an unknown chromosomal location in the reference genome). Chromosomes 1H and 3H contained one gene each of *HvADC1* and *HvPAO5*, respectively. Chromosome 4H contained two genes (*HvPAO1* and *HvCuAO2*), while all other *Hv*PMG genes were located on the chromosomes 2H, 5H, 6H and 7H. Gene duplication analysis revealed 8 (34%) *Hv*PMG duplicated genes in barley chromosomes. Among them, two gene pairs had tandem duplication and six gene pairs segmental duplication (Supplementary Tables S7 and S8). The tandemly duplicated genes (*HvPAO6*/ *HvPAO3* and *HvPAO7*/ *HvPAO8*) were located tandemly at a single locus on chromosome 2H and 7H, respectively. Segmentally duplicated *Hv*PMG gene pairs were located on chromosome 2H, 4H, 5H, 6H and 7H, whereas no gene duplication event was found on chromosomes 1H and 3H.

Next, we explored the selective constraints on the duplicated genes to determine molecular evolutionary rate of duplicated *Hv*PMG genes. The ratio of non-synonymous substitution (Ka) and synonymous substitution (Ks) was used to examine the selection pressure among duplicated gene pairs. Values of Ka, Ks and Ka/Ks for each paralogous gene pair were calculated (Supplementary Table S9). The Ka/Ks values for *Hv*PMGs were 0.106 and 0.98, respectively, for the two tandem duplication genes (Supplementary Table S7) whereas Ka/Ks value ranged from 0.069–0.723, with an average value of 0.291, for segmentally duplicated genes (Supplementary Table S8). Also, divergence periods for segmental and tandem duplicated gene pairs in barley were estimated. The estimated divergence time was about 82.490 MYA for tandem duplicated genes and 51.48 MYA for segmental duplicated gene pairs. The divergence of gene pairs *HvPAO7*/ *HvPAO8* and *HvCuAO2*/ *HvCuAO3* seems to have occurred about 145.586 MYA and 16.265 MYA, respectively.

4. Cis **-acting regulatory elements, miRNA target sites prediction, and protein-interaction analysis**

To identify the *cis*-acting regulatory elements (CREs) in the promoter regions, the 1000 bp upstream sequences of *Hv*PMG genes were retrieved from the database of *H. vulgare* genome and analyzed using PlantCARE. A total of 961 putative CREs were identified (Fig. 3A). The identified *cis*-elements were further divided into five groups: 145 elements which were related to hormone response, 260 elements associated with stress response, 140 elements related to light response, and 385 elements associated with growth and development. Thirty elements remained uncharacterized. CREs for growth and development were of 21 types among which CAAT-box and TATA-box were the most abundant elements, 143 and 145, respectively, - commonly shared by most of the *Hv*PMG genes. Also, 22 different types of members were found in light responsive elements, mainly, I-box, Sp1, G-box, GT1-motif, Box 4 and G-Box. Comparatively, 11 types of elements related to hormone response. These are ABRE involved in abscisic acid (ABA) response, TCA/TCA-element in salicylic acid response, CGTCA-motif and TGACG-motif in jasmonic acid (MeJA) response, TGA-element and AuxRR-core in auxin response, and ERE in ethylene response. Additionally, stress responsive elements comprised STRE, LTR (low temperature response), MBS for drought inducibility, TC-rich repeat for defense/stress response, WUN-motif for wound response, and ARE and GC-motif for anaerobic induction. Notably, circadian-related CRE was associated with the promoter regions of two *Hv*PMG genes.

A total of 9 *H. vulgare* miRNAs (hvu-miR) comprising target sites in 9 *Hv*PMG genes were identified (Table 3). The miRNA target sites were mainly identified in amine oxidases. Two amino oxidase genes had more than one target sites, *HvCuAO6* was targeted by three miRNAs (hvu-miR5049b, hvu-miR6180 and hvu-miR6210), and *HvPAO7* by two (hvu-miR6196, hvu-miR6206). Three miRNAs, hvu-miR6196, hvu-miR6180 and hvu-miR6187, had two target sites each in different *Hv*PMGs. *HvADC1*, *HvSPDS1* and *HvSAMDC1* were targeted by hvu-miR6196, hvu-miR6180 and hvu-miR6185, respectively. No target sites were identified in *HvODC* genes. Almost all of the identified miRNA-targeted *Hv*PMG genes were predicted to be silenced by cleavage inhibition, except for hvu-miR5049b. To represent the target accessibility, energy required to unpair the secondary structure around target site (UPE) was also calculated by RNAup[45]. The results indicated that the UPE varied from 12.44 (hvu-miR6196) to 22.629 (hvu-miR6187).

Table 3
The potential miRNA target sites in barley polyamine metabolic pathway genes. *ADC* (arginine decarboxylase); *SAMDC* (S-adenosylmethionine decarboxylase); (spermidine synthase); *SPMS* (spermine synthase); CuAO (Diamine or copper-containing oxidase); and *PAO* (polyamine oxidase) in barley (*Hv*).

miRNA Acc.	Target Acc.	Expectation	UPE	miRNA length	Target start-end	miRNA aligned fragment	Target aligned fragment	Inhibiti
hvu-miR5049b	*Hv*CuAO6	3.5	12.597	21	2003–2023	AGUAUUUAGGUACAGAGGGAG	CUCCCUCCGUUCCUAAAUACA	Transl
hvu-miR6196	*Hv*ADC1	3.5	12.44	21	1361–1381	AGGACGAGGAGAUGGAGAGGA	ACCUCUCCAUCUUCUCGCUCG	Cleava
hvu-miR6180	*Hv*CuAO6	4.5	15.222	20	171–190	AGGGUGGAAGAAAGAGGGCG	UGCGUACUUUUUUCCACCAU	Cleava
hvu-miR6187	*Hv*PAO4	4.5	19.169	21	705–725	UGAACAGGUUCGGCGACCUCA	CAGGGUUGUUGAAAUUGUUCG	Cleava
hvu-miR6199	*Hv*PAO8	4.5	17.272	23	249–271	CCACAGAAUUCUCACAGUGAUGG	UGUUUGCAAUGAGAAUUCUUUGG	Cleava
hvu-miR5049c	*Hv*PAO6	5	17.561	23	1232–1254	AGACAAUUAUUUUGGGACGGAGG	UCCUCGUGCCGAGGUGGUGGUCU	Cleava
hvu-miR6180	*Hv*SPMS1	5	19.654	20	1020–1039	AGGGUGGAAGAAAGAGGGCG	AGCGUUUGUUCUUCCAACCU	Cleava
hvu-miR6185	*Hv*SAMDC1	5	22.006	21	1309–1329	UCUGGCAGCGACGGGAACAUA	AAAGAUGUCGUCGCUGCCUGA	Cleava
hvu-miR6187	*Hv*CuAO4	5	22.629	21	374–394	UGAACAGGUUCGGCGACCUCA	GCAUGGCGUCGGAGCUGUUCG	Cleava
hvu-miR6196	*Hv*PAO7	5	19.803	21	122–142	AGGACGAGGAGAUGGAGAGGA	UCCUCUCCAACUCCUCUUUUG	Cleava
hvu-miR6206	*Hv*PAO7	5	24.273	22	105–125	GGCACACGGGCUGCAGGCAUAG	GAUUGCC-GCGGCUCGUGUCCU	Cleava
hvu-miR6210	*Hv*CuAO6	5	15.205	22	1472–1493	ACUCCUUGGUUAUCAACUUCGA	AUGAAGCUUAUAAUCAGGUGGU	Cleava

The protein interaction analysis was carried out on STRING webtool with a maximum of 20 interactions. Out of a total 23 *Hv*PMG proteins, 18 showed protein-interactions (Fig. 3B) while HvPAO1, HvPAO6, HvPAO7, HvODC1 and HvCuAO2 did not show any interaction. The protein interactions were further analyzed using kmeans clustering. Proteins clustered in three clusters (Supplementary Table S10), Cluster 1 contained 18 members including amine oxidases (HvPAOs and HvCuAOS); Cluster 2 contained 9 proteins including HvADC1 and HvODC2; and Cluster 3 contained 11 proteins including HvSAMDCs and HvSPDS/SPMS genes. In Cluster 1, the barley amine oxidases indicated interaction with MLOC_12946.1 (aldehyde dehydrogenase family), MLOC_17787.2 (Aldedh domain-containing protein) and MLOC_34526.1 (aldehyde dehydrogenase family). In Cluster 2, HvODC2 and HvADC1 had interactions with MLOC_35821.1 (ornithine aminotransferase), MLOC_61790.1 (Cn hydrolase domain-containing protein) and MLOC_65968.1 (arginase family) proteins. The cluster 3 proteins showed interactions with MLOC_15895.1 (PNP_UDP_1 domain-containing protein), MLOC_64689.1 and MLOC_65908.2 (Aminotran_1_2 domain-containing proteins) and MLOC_80387.3 (S-adenosylmethionine synthase 4).

5. Database search for expression analysis of barley polyamine metabolic genes

Gene expression data of various tissues and developmental stages of barley were obtained by using publicly available gene expression databases, namely, mRNA-Seq Gene Level Hordeum vulgare (ref: Morex V3) and Affymetrix Barley Genome Array on GENEVESTIGATOR. Among all the 23 *Hv*PMGs, the expression data of only 19 genes was found, and many of these genes had a distinct tissue-specific expression (Fig. 4A). Thus, *HvADC1* was highly expressed in seedling, preferentially in shoot, root tip, elongation zone and maturation zone; *HvPAO6* was highly expressed in root tip, elongation zone, maturation zone and seedling; and *HvPAO1* was preferentially expressed in lodicule, rachis and palea tissues. *HvSAMDC3* gene was highly expressed in almost all the tissues, while *HvODC1*, 2 had very low expression in most of the tissues. Genes *HvSPDS1*, *HvSPMS1* and *HvCuAO7* were differentially expressed in various tissues. Next, we analyzed gene expression of barley *Hv*PMG genes at eight developmental stages, namely, germination, seedling, tillering, stem elongation, booting, flowering, milk and dough stage (Fig. 4B). All the *Hv*PMG genes were expressed at the germination stage, except for *HvODC1* (at seedling stage), *HvCuAO6* (at booting stage), *HvPAO1* (at stem elongation stage) and *HvPAO*2 (at seedling stage). *HvPAO3*, *HvPAO6*, *HvODC1* and *HvODC2* were expressed until seedling stage while no expression was observed at the later stages. Many genes such as *HvCuAO7*, *HvSAMDC3*, *HvPAO4* and *HvSPMS1* were expressed at all the developmental stages. These data indicate a correlative gene expression pattern of *Hv*PMG genes, particularly during developmental stages.

Expression of *Hv*PMG genes was found to significantly respond to various stress conditions (Fig. 4C). Thus, *HvADC1* was up-regulated under heat, drought, salt and simulated drought stress conditions while *HvSAMDC2* was slightly up-regulated in simulated drought and cold stress conditions. Tissue specific expression of *HvPAO2* gene under stress (drought) was down-regulated in spikelet but up-regulated in the leaf and spikes. The genes *HvPAO3* and *HvPAO6* were down-regulated under heat and simulated drought conditions. *HvPAO8* was down-regulated under simulated drought and cold conditions, while *HvSAMDC1* was down-regulated under simulated drought, salt, osmotic and drought conditions.

6. Organ-specific expression analysis of polyamine metabolic pathway genes

Organ specific gene expression in barley root, shoot, leaf, stem and coleoptile was quantified using qRT-PCR with ACTB (actin) AY145451 as an internal reference and the results were normalized against the coleoptile tissue expression (Fig. 5). Expression of *HvSAMDC1*, *HvPAO6* and *HvPAO3* was significantly higher in roots as compared to other tissues such as coleoptile, shoot and leaf; expression of *HvPAO4, HvSAMDC2* and *HvSPMS1* was higher in the leaf while *HvSAMDC3* was highly expressed in the stem. In contrast, *HvSPMS2* expression was lower in root and shoot, and *HvPAO8* had a similar expression profile across all the tissues. The expression of the remaining five barley PA metabolic pathway genes (*HvADC1, HvCuAO3, HvCuAO7, HvPAO2* and *HvPAO7*) was low in root, shoot, leaf and stem as compared to that of the coleoptile.

7. Polyamine metabolic pathway genes expression analysis in dark-induced leaf senescence

Dark-induced leaf senescence (DILS), in the form of severe shading or darkening of leaves, induces leaf senescence similar to that observed during normal plant development. DILS has been utilized as a model to study early and late events in barley leaf senescence[46,47]. In this study, DILS involved keeping the plants in darkness and then assessing expression of 12 genes of HvPMGs at 0, 3, 7 and 10 days (Fig. 6). The gene expression was quantified using *H. vulgare* pyruvate kinase family protein gene (AK356185) as the reference gene for senescing barley leaves [48]. A control was run along with similar timepoints to eliminate the possibility of variation of genes expression during normal condition. In control conditions, the expression of *HvSAMDC2, HvSAMDC3, HvPAO2, HvPAO4* and *HvPAO7* was upregulated at all stages. Notably, *HvSPMS2* expression was highly upregulated with 12-fold expression on day-10 as compared to day-0. The expression of the rest of the six other genes remained unchanged throughout the growth under normal conditions. An early transient response was observed in the expression of *HvSPDS1, HvSPMS1* and *HvSPMS2* genes at day-3 in dark, which further decreased as the senescence progressed. The expression of *HvCuAO3* and *HvCuAO7* was upregulated during senescence till day-7, with a decline thereafter. In contrast, *HvPAO7* and *HvPAO8* expression was upregulated as the senescence progressed, being highest at day-10. Notably, *HvPAO2* did not express in the dark, while expression of HvPAO4 remained unchanged during dark incubation. The remaining three genes (*HvSAMDC2, HvSAMDC3* and *HvADC1*) followed a similar expression pattern as under normal conditions. Comparing control versus dark at each timepoint, *HvSPDS1* and *HvSPMS1* were significantly upregulated at day-3 and day-7, *HvSPMS2* was downregulated while *HvPAO8* was upregulated at day-10. Also, *HvSAMDC2* was upregulated at day-7 and then downregulated at day-10.

Discussion

Polyamines metabolism genes have been identified and studied in a few plant species, including Arabidopsis, rice and tomato[20,49–55]. Here, we have presented a systematic investigation of PMGs at a whole-genome scale in barley. Genes involved in polyamine metabolic pathway in barley were identified and characterized together with their comparative assessment in relation to those known in Arabidopsis, rice and maize. Polyamine metabolism enzymes involved in the synthesis and catabolism of free PAs pool in plant cells are shown in Fig. 7.

We have identified three *SAMDC*, two *ODC*, one *ADC*, one *SPDS*, two *SPMS*, five *CuAO* and seven *PAO* members (in addition to the previously reported two PAOs[56]) in barley. The PA metabolic genes *ADC*, *ODC*, *SPDS* and *SPMS*/*tSPMS* in plants are highly conserved among different species, and they typically have only two copies each, except one copy each of *SPMS* and *tSPMS*[49]. In animals, the ODC pathway is considered essential in PA biosynthesis as almost all eukaryotes synthesize Put directly from ornithine (Orn) in a reaction catalyzed by ODC. The ODC pathway is present in most of the plant species, except for some species of the Brassicaceae, with ODC being absent in Arabidopsis[57]. During the early evolution of Brassicaceae, two paralogs (ADC1 and ADC2) of ancestral ADC gene were generated by duplication event and retained even after the genome shrinkage in species such as Arabidopsis[58]. The duplication of ADC genes might be a compensatory mechanism for the absence of ODC in plants[57]. Hence, ODC pathway is likely not essential for plants as ADC pathway does the same function. In the analysis presented here, both the *ODC* and *ADC* genes were identified in barley along with their developmental or stress specific function. Presence of many family members of isoforms indicates major contribution of gene duplication to functional diversity in higher organisms[59]. The number of PA metabolic pathway genes varies among species, implying that duplication events have occurred during the evolution of different species or due to their different genome size. Similarly, in barley as well it could be due to both, large genome size or an evolutionary process.

The biosynthetic pathways for PAs are conserved among organisms, from bacteria to animals and plants[14]. To delineate the comparative phylogenetic relationship of PA metabolic pathway genes in barley with other plant species, our phylogenetic analysis demonstrated that PA metabolic pathway proteins are highly conserved in the four species; barley, Arabidopsis, rice and maize, with the SAMDCs, PAOs, CuAOs, ADCs, ODCs, and SPDS/SPMSs being clustered into one group, respectively. The PA metabolic pathway protein sequences had homologues regions and shared the conserved catalytic active sites with other plant species; SAMDCs[60], PAOs[56], CuAOs[33], ODCs and ADCs[34]. The SPMS/SPDS protein sequences were highly similar and also shared conserved active regions[35,36]. The *SPDS* and *SPMS* were found not distinct from one another. *AtSPMS* in the Arabidopsis genome is also designated as *AtSPDS3*. Thus, the *HvSPMS* genes identified in barley can also act as *SPDS*. This analysis confirmed that the PA metabolic pathway is highly conserved in plants.

Plant PAOs are classified into two groups, terminal catabolism (TC) reaction-type and back-conversion (BC) reaction-type. The TC-reaction produces 1,3-diaminopropane (DAP), H_2O_2, and the respective aldehydes, while the BC-reaction produces Spd from tetraamines, Spm and T-Spm and/or Put from Spd, along with 3-aminopropanal and H_2O_2[37]. Previous studies on phylogenetic relationships showed that plant polyamine oxidases (*PAOs*) can be classified into four clades[20,38,39]. Our study revealed that barley genome contains nine genes coding for polyamine oxidase (*PAO*) with members classifying into clades II, III, and IV but not into clade-I (Supplementary Fig. S13). Plant *PAOs* belonging to clade-I seem to catabolize PAs in the BC-type reaction and are localized in the cytoplasm. As none of the barley *PAOs* belongs to clade-I, it can be assumed that barley PAOs do not have this characteristics with respect to reaction type and localization. The clade-III *PAOs* are also involved in degradation of PAs in the BC reaction and found to be localized in cytoplasm[37,40,61]. One barley *PAO* gene (*HvPAO5*) falls into this group. Furthermore, clade-III genes of Arabidopsis and rice are intron-less genes[37,61,62], so is the *HvPAO5*. The Arabidopsis member of clade-III, *AtPAO5*, has been extensively characterized[61]. Phenotypes of *AtPAO5* knock-down mutants (*At*pao5) have also higher T-Spm contents

than wild-type plants. In our analysis of barley, thermospermine synthase-like (*tSPMS*/ *ACULIS5*-like) gene was not identified. The evolutionary studies of PAO genes in this clade might be of interest since these genes are intron-less and code for T-Spm specific PAOs. Clade-IV members are also of BC-type but are localized in peroxisomes[38,63,64]. Three barley *PAOs* (*HvPAO4*, *HvPAO7* and *HvPAO8*) belong to this clade, suggesting that they play similar roles as clade-IV members of other species. The clade-II members catabolize PAs differently in the TC-type reaction, and localize either in the vacuole[41,65] or in the apoplast[37,66,67]. In barley, five *PAOs* (*HvPAO1*, *2, 3, -6* and *– 9*) belong to clade-II type *PAOs*. In previous reports, barley *HvPAO1* and maize *ZmPAO1* (Clade-II *PAOs*), were found to be induced by wounding[68], while rice *OsPAO6* was upregulated by JA (jasmonate) treatment[67]. It seems that these *PAOs* (clade-II) originated from monocotyledonous plants, since they are not found in dicot plants such as Arabidopsis and tomato[39]. Thus, barley has both BC-Type and

TC-Type *PAOs*, whereas Arabidopsis and tomato plants do not contain clade-II TC-type *PAO*(s).

The gene duplication events (tandem/segmental) in plants are considered to be one of the main driving forces in the evolution and expansion of the gene family, and in the establishment of new protein functions[69]. Gene duplication analysis in this study revealed the tandemly and segmentally duplicated *Hv*PMG genes. The *Hv*PMG genes without duplicated sequences might have originated from different progenitors. The occurrence of the genes at the same chromosomal location implies a common origin, from which they might have evolved by a series of duplication events[70]. The gene duplication analysis suggests that tandem and segmental duplications may have played an important role in the expansion and evolution of the *Hv*PMG gene family in plants, resulting in their structural and functional diversification. In genetics, the Ka/Ks ratio is used as an indicator of selective pressure acting on a protein-coding gene. In our study, the Ka/Ks ratios of all duplicated *Hv*PMG gene pairs were less than one, which supports that evolution of genes may have occurred from intensive purifying selection pressure by natural selection during the evolutionary process. These results are consistant with the other evolutionary studies carried out in barley[71,72]. In addition, the estimated divergence time for *Hv*PMGs in barley was found to be about 87.90 MYA for tandem duplicated genes and 54.85 MYA for segmental duplicated gene pairs. The majority of gene pairs were found to have diverged long before the divergence time of grass species (56–73 MYA)[73,74]. Barley and Arabidopsis share a common ancestor but they have diverged considerably since their separation around 140 million years ago. This could be attributed to structural difference in barley and Arabidopsis PMG genes[75,76]. The gene pair *HvPAO7*/ *HvPAO8* diverged at 145.5864 MYA during the emergence of monocot and dicot plant species (140–150 MYA)[76]. Although the gene pair (*HvCuAO2*/ *HvCuAO3*) may represent a newly duplicated gene pair as it was estimated to diverge about 15.26 MYA, yet all the duplicated gene pairs were estimated to have originated before the divergence of the genus *Hordeum* (12–13 MYA)[73,77]. This indicates that the expansion of the *Hv*PMG gene family in barley may be associated with gene duplication events.

The potential regulatory mechanisms controlling *Hv*MPG gene expression both by analyzing the *cis*-regulatory elements (CREs) and the microRNA target sites in the promoter regions and the coding sequences of *Hv*PMG genes were, respectively, explored. The variation of CREs is critical for phenotypic evolution in all organisms. In plants, broadly, regulatory regions are enriched for loci associated with phenotypic variation, for example, in maize[78,79] and rice [80,81]. Thus, analysis of CREs is critical to understanding the relationship between phenotype and genotype as they often dictate genes' spatio-temporal expression[82]. Here, a total of 961 putative CREs were identified in the promoter regions, the 1000 bp upstream sequences, of *Hv*PMG genes. Among all the identified CREs, CAAT-box and TATA-box in the group growth and development appeared to be the most abundant CREs and were commonly shared by most of the *Hv*PMG genes. These elements are believed to determine the efficiency of transcription[83], as CAAT-box is a common cis-acting element in promoter and enhancer regions, and TATA-box is a core promoter element around − 30 of transcription start site. Among others, some of the regulatory elements for stress response (MYB, MYC and STRE), light response (G-Box and GT1-motif) and hormone response (ABRE, CGTCA-motif and TGACG-motif) were common in most of the *Hv*PMGs. The presence of a well conserved TATA-box and other putative cis-acting motifs responsive to light or auxin (G-box, AuxRE-box, TGACG-box and CCAAT-box) in promoter regions of two maize PAO genes are known[84]. Thus taken together, our results on the identification of *cis*-regulatory elements indicate that *Hv*PMG genes could be transcriptionally regulated by multiple stimuli, and may participate in various plant metabolic processes as well as spatio-temporal expressions of identified isogenes.

A total of 9 *H. vulgare* miRNAs (hvu-miR) comprising target sites in 9 *Hv*PMG genes were identified. The accessibility of the mRNA target site to small RNA has been identified as one important factor involved in target recognition. The UPE value representing the target accesibility in this study indicated a better miRNA-target binding[85]. The target mRNAs show almost-perfect or imperfect complimentarity with the miRNA in terms of mRNA cleavage or miRNA-direct translational inhibition, respectively[86,87]. In plants, miRNAs have been shown to be involved in various biotic (bacterial and viral pathogenesis) and abiotic stress responses such as oxidative, mineral nutrient deficiency, drought, salinity, temperature and cold[88–90]. Many reports have shown that miRNAs regulate responses of barley to different stress conditions[90–93]. Previous studies have shown that some of the identified miRNAs in this study were involved in both abiotic and biotic stress responses. For example, miRNA hvu-miR5049b is up-regulated under drought conditions [Hackenberg et al.[94], while upregulation of hvu-miR6196 occurs during salt adaptation of the autopolyploid *Hordeum bulbosum* [Liu et al.[95], and differential expression of hvu-miR6180 fungal stress in wheat has also been reported [Inal et al.[96]. Thus, exploring the role of miRNAs in HvPMG gene functions in response to various stresses would be of great interest.

The regulatory PPI network for the barley PA metabolic pathway genes indicated considerable interactive networks among the proteins involved in aldehyde dehydrogenase family, Aldedh domain-containing protein, ornithine aminotransferase, Cn hydrolase domain-containing protein, arginase family, PNP_UDP_1 domain-containing protein, Aminotran_1_2 domain-containing proteins, and S-adenosylmethionine synthase 4. Many of these proteins were previously shown to be involved in plant development and stress responses. For example, aldehyde dehydrogenases (ALDH), a family of enzymes involved in plant metabolism and aldehyde homeostasis to eliminate toxic aldehydes, are expressed in response to stress conditions such as high temperature, high salinity, dehydration, oxidative stress, or heavy metals in Arabidopsis[97], *S. tuberosum* and *N. benthamiana*[98], and other plant species[99,100].

In plants, the expression of gene isoforms varies depending upon the plant tissue, developmental stage and environmental conditions[101]. The gene expression analysis in this study revealed that many *Hv*PMGs are expressed in a redundant manner in different tissues during developmental stages in barley, supporting

the idea that PA metabolism genes are involved in various tissues during all developmental processes in all living organisms[17,102,103]. The expression of *HvODC1 and 2* was found only in roots which suggests that barley plants utilize the ODC pathway to produce Put only in roots, while in other organs the alternate ADC pathway is active. *HvSAMDC3*, *HvCuAO7, HvPAO4* and *HvSPMS1* were expressed in all the developmental stages indicating that they are involved in processes related to plant growth and development. Our results with barley are consistent with other studies of PA metabolism genes. The fact that *HvADC1* was up-regulated during heat-drought, salt and simulated drought stress condition while *HvSAMDC2* was slightly up-regulated in simulated drought and cold stress conditions is indicative of the fact that PA metabolism genes play an important role in responses to various abiotic stresses. This is consistent with the presence of putative *cis*-acting elements in the promoter region of PA biosynthetic genes including *ADC* and *SAMDC*.

It is known that PAs are anti-senescence in nature[104]. One such validation has come from genetic dissection of leaf senescence models, including dark-induced leaf senescence[46,105,106]. These studies indicate that PA catabolism can play a central role in metabolic reprogramming, directing a senescing leaf toward programmed organ death. Thus, depending upon which direction PA metabolism takes, synthesis/accumulation or catabolism that generates H_2O_2, the plant will either grow or senesce, respectively. DILS is a barley crop model for early and late events as well as for the identification of the critical time limit for reversal of the senescence process that prevents leaves from reaching the cell death phase. The efficiency of regulation of the senescence process is a sign of the vitality of senescing cells, which at each stage must maintain their ability to maintain homeostasis[46,47,106]. A critical moment in the model that determines the point of no return has been identified[46] but the mechanism of its control is still unknown. Some suggestions regarding the PA metabolism gene expression pattern in senescing leaf have been provided by microarray data[106]. The leaf senescence-associated changes in gene transcripts involved in PA metabolism were also a part of the present study. Clearly, expression of *SPDS/SPMS* gene family transcripts' in barley leaf during senescence showed significant changes. The data presented in this study suggests that the *HvSPDS1, HvSPMS1, HvSPMS2* and *HvSAMDC2* gene isoforms involved in the biosynthesis of PA metabolism are the key genes in polyamine metabolism that may condition senescence-dependent metabolic reprogramming. Interestingly, *HvPAO8*, involved in the catabolism of PAs, responded significantly during senescence and the phylogenic study showed that *HvPAO8* is also a back-conversion type gene. Whether *HvPAO8* is active in back-conversion during the senescence process remains to be determined. Interestingly, a correlation between the levels of *HvPAO8* and *HvSPMS2* transcripts and dark-induced leaf senescence was detected in this study and needs to be further tested.

Genetic mechanisms that lead to stress-induced senescence and delineate processes involved in either delaying or accelerating senescence are important to be deciphered. Development of transgenic barley plants that are defective in specific PA metabolic genes need to be generated via the ubi-overexpression, RNAi approaches or CRISPR/Cas9[107–109]. This should allow gaining "anti-aging" or "pro-aging" phenotypes as an important intervention. Designing a strategy to systematically knockout the genes involved in the biosynthesis, degradation and sequestering of PAs could provide an array of plants with different senescence phenotypes. In order to have plants that can be grown without restrictions under field conditions, one possible alternative is to select promising CRISPR/Cas9 mutations and mimic them by TILLING screening of a classical mutant collection.

Conclusions

Polyamine metabolic pathways genes in barley were identified and characterized at a whole-genome scale to provide an insight into their genomic and structural organization, regulatory framework, physicochemical properties, phylogenetic and evolutionary relationships, and expression profiles during developmental stages in different tissues and under abiotic stresses with special emphasis on induced leaf senescence. This study is the first to systematically and comprehensively analyze the PAs metabolic pathway gene families in barley. Our results not only extend novel findings but also provide valuable information about Gramineae crop development, their stress physiology, and future prospects for genetic improvement programs associated with PAs. There is a need for deeper understanding of plant biology vis a vis crop improvement related to PAs regulation, which can progress further through molecular tools, such as PA omics profiling and genetic engineering, and lead to the development of novel germplasm.

Methods

1. Identification of polyamine metabolic pathway genes in barley and physiochemical characterization of proteins

Genome sequence from *Hordeum vulgare (IBSC_v2)* hosted at EnsemblPlants database (https://sep2019-plants.ensembl.org/Hordeum_vulgare/Info/Index) was utilized to retrieve putative barley (*H. vulgare*) polyamine metabolic pathway gene transcripts and protein sequences. Multiple bioinformatics approaches were employed to identify and characterize potential genes in barley as described by Upadhyay and Mattoo [110]. PA metabolic pathway encoding sequences for arginine decarboxylase (*ADC*), ornithine decarboxylase (*ODC*), S-adenosylmethionine decarboxylase (*SAMDC*), polyamine oxidase (*PAO*), copper-containing oxidase or diamine oxidase (C*uAO*), spermidine synthase (*SPDS*) and spermine synthase (*SPMS*) from *Arabidopsis* gene annotation database (TAIR) and rice database (https://www.plantgdb.org/OsGDB/) were downloaded and used as a query against barley genome to search for similar sequences. BLASTp search (E value, 10^{-5}) was used to search for similar protein sequences in barley genome. Putative PA pathway protein sequences of barley were analyzed using Hidden Markov Model (HMM) analysis for the presence of a typical HMM domain representing the corresponding protein class in a HMMER search (https://www.ebi.ac. uk/Tools/hmmer/)[110,111]. For accuracy these sequences were also cross verified with InterProScan[112], and the candidates containing any of the typical domains of respective proteins were recognized as PA metabolic proteins. Gene nomenclature was based on their occurrence on pseudomolecules. Characteristics of each of the identified barley PA metabolic pathway proteins such as isoelectric point (pI), amino acid sequence length (AA), molecular weight (MW) and grand average of hydropathicity (GRAVY) were obtained using tools available at the ExPASy bioinformatics resource portal (https://www.expasy.org). The3 sub-cellular localizations were predicted by Plant-mPLoc webtool (http://www.csbio.sjtu.edu.cn/bioinf/plant-multi/) and putative transmembrane regions were predicted by using the TMHMM Server V. 2.0 (https://services.healthtech.dtu.dk/service.php?TMHMM-2.0). In addition, N-terminal transit/signal peptide prediction was obtained using the webserver (https://services.healthtech.dtu.dk/service.php?TargetP-2.0).

For PCR amplification of each identified and extracted gene sequence in barley, the gene-specific primers were designed by Primer-BLAST web-server (https://www.ncbi.nlm.nih.gov/tools/primer-blast/). The DNA was isolated from the leaves of 10-day-old (grown at day/night 16/8 h, light intensity 300 µmol m^{-2} s^{-1}) barley plants using Genomic Mini AX PLANT kit (A&A Biotechnology). The chosen regions in the extracted gene sequences were amplified by PCR (Thermo Scientific Phusion Green Hot Start II High-Fidelity DNA Polymerase) in lab and confirmed by sequencing the PCR products (outsourced at NEXBIO Sp. z o. o, Lublin, Poland). Primers used in this analysis are listed in Supplementary Table S11.

2. Gene structure, protein sequence alignment and phylogenetic analysis

Sequences from model plants, namely, Arabidopsis, rice, and maize were selected for analyzing *ADC*, *ODC*, *PAO*, *CuAO*, *SAMDC*, *SPMS* and *SPDS* genes. For gene structure analysis, genomic DNA and coding DNA sequences corresponding to each identified gene were analysed**.** The GFF3/GTF annotation file containing the locations of PA metabolic pathway genes in genome and their structural information was extracted from the EnsemblPlants database (https://plants.ensembl.org/index.html) and the exon-intron structure was displayed using the GSDS2.0 Gene Structure Display Server (http://gsds.cbi.pku.edu.cn). The MEME tool from the MEME suite 5.3.3 (http://meme-suite.org/tools/meme) was used to identify ten statistically significant motifs in the protein sequences based on "zero or one occurrence per sequence (zoops)". Hidden Markov Model analysis was done with HMMER database by Inter-pro scan program hosted at webtool (http://www.ebi.ac.uk/interpro/).

Multiple sequence alignments were performed using the ClustalW program with default settings. The conserved regions and catalytic active residues in multiple sequence alignments were visualized on Jalview software[113]. The JPred Secondary Structure Prediction [114] in the Jalview software was used to predict the secondary structures as well as the presence of structural elements in the PA metabolic pathway protein sequences. A phylogenetic tree was constructed using the Neighbor-Joining method with Poisson correction and 1000 bootstrap values using the MEGA-11 program[115], while the tree was visualized on iTOLv6 program (https://itol.embl.de/). The evolutionary distances were computed using the p-distance method and are in the units of the number of amino acid differences per site. All ambiguous positions were removed for each sequence pair (pairwise deletion option). Evolutionary analyses were conducted in MEGA-11[115].

3. Chromosomal location, gene duplication and evolutionary rate calculations

Chromosomal distributions of barley PA metabolic pathway genes (*Hv*PMGs) were determined according to the genome annotation GFF3/GTF files (https://plants.ensembl.org/Hordeum_vulgare/Info/Index) and visualized by TBtools software [116]. Gene duplication events were analyzed by using Multiple Collinearity Scan toolkit (MCScanX) with the default parameters[117] and gene duplication events were drawn by TBtools software[116]. The number of synonymous (Ks) and non-synonymous (Ka) substitutions per site of duplicated gene pair were calculated by TBtools software. Based on a rate of 6.5×10^{-9} substitutions per site per year, the divergence time (T) was calculated as $T = Ks/(2 \times 6.5 \times 10^{-9}) \times 10^{-6}$ MYA for monocots[118-121].

4. Cis-acting regulatory elements, miRNA target sites prediction and protein interaction analysis

The promoter sequences (1000 bp up-stream) of barley PA metabolic pathway genes were retrieved from *H. vulgare* genome database (https://plants.ensembl.org/Hordeum_vulgare/Info/Index). The obtained sequences were then uploaded in PlantCARE database (http://bioinformatics.psb.ugent.be/webtools/plantcare/html/) for *cis*-acting regulatory elements analysis[122]. The coding sequences of barley PA metabolic pathway genes were analyzed by psRNATarget server (https://www.zhaolab.org/psRNATarget/) for miRNA target sites prediction[123]. The protein interaction analysis was carried out on the STRING webtool (https://string-db.org/)[124]. The maximum numbers of interactions were restricted to no more than 20 and clustering was done as per kmeans clustering.

5. Database search for expression analysis of barley polyamine metabolic pathway genes

The expression patterns of PA metabolic genes during various developmental stages were analysed using Gene Expression Atlas of EMBL-EBI at http://www.ebi.ac.uk/gxa/[125] for barley. The expression data were downloaded as TPM values and Z-score was calculated using the logTPM values. The expression in different organs and under abiotic stress conditions was carried out using mRNA-Seq Gene Level Hordeum vulgare (ref: Morex V3) and Affymetrix Barley Genome Array on GENEVESTIGATOR v3 tool[126,127]. The expression data was visualized and heat maps were generated using the TBtools software [116].

6. Gene expression analysis of barley polyamine metabolic pathway genes

The organ-specific expression of barley PA metabolic pathway genes in root, shoot, leaf, stem, coleoptile and seedlings was checked as described below.

Plant material and growth conditions: Barley seeds were surface sterilized, soaked for 1 h in tap water and germinated in the dark in moistened soil in pots. Three days old etiolated seedlings were transferred to growth chamber under controlled conditions (day/night 16/8 h, light intensity 300 µmol m^{-2} s^{-1}) and the seedlings after four days of growth were taken as day 0 for all the experiments. The plant samples (root, shoot, leaf, stem, coleoptile and seedlings) were harvested separately, washed thrice with distilled water, frozen in liquid nitrogen and stored at -80 °C until used. The plant material was collected according to the institutional, national, and international guidelines and legislation. All the experiments were performed in accordance with relevant guidelines and regulations.

Experimental senescence model. Dark-induced leaf senescence of barley described previously[46] is a useful model to study induced senescence. The experiments were carried out on barley first leaf. Barley (*Hordeum vulgare* cv. Golden Promise) seedlings were grown as described above. Senescence in 7-day-

old seedlings was induced by darkness which lasted from 0 to 10 days. The leaf samples from day 0 (control), 3, 7 and 10 were harvested for analysis. The control plants were grown continuously under the photoperiod. The control plants were also a variant of barley early developmental stages. All experiments were carried out in triplicate.

RNA Extraction and qRT-PCR: Total RNA was extracted from 100 mg of each sample using the Thermo Scientific GeneJET Plant RNAPurification Mini Kit (K0801) and DNA contamination was removed by using Thermo Scientific RapidOut DNA Removal Kit (K2981). RNA samples with an $A_{260/280}$ ratio of 1.8-2.0 were then electrophoresed on agarose gels to ensure the presence of intact rRNA bands. A RevertAid H Minus First Strand cDNA Synthesis Kit (Thermo Scientific, K1632) was used to synthesize the first strand cDNAs from the mRNAs (1 ug). Organ specific expression analysis of barley PA metabolic pathway genes was carried out by qRT-PCR on QuantStudio™ 3 Real-Time PCR System (Applied Biosystems™) using PowerUp™ SYBR™ Green Master Mix (Applied Biosystems). The gene expression ratio was calculated using the method by Pffafl [128]. qRT-PCR data represent the average±standard deviation of a minimum of two independent biological replicates for each gene. The gene-specific primers were designed by Primer-BLAST web-server (https://www.ncbi.nlm.nih.gov/tools/primer-blast/). Each primer sequence was tested with a blast search in the genome of barley for specific hits and for its specificity to yield a single amplicon on 3% agarose gel. Primers used in this analysis are listed in Supplementary Table S12.

7. Data analysis

The GraphPad (version 9.3.1) suite was used for statistical analysis. ANOVA with Dunnett's multiple comparisons test was performed for significant differences in the organ specific gene expression analysis. Statistical significance between data points was assessed against coleoptile (Cl) versus expression profiles of other organs. For the DILS analysis, ANOVA with Bonferroni's multiple comparisons test was performed for significant differences. Statistical significance between data points was assessed against day-0 (control) timepoints versus other timepoints of expression profiles (day-3, 7 and 10), and also for each timepoint in light versus dark. The statistical significance was categorized as *P<0.05, **P<0.01, ***P<0.001 and ****P<0.0001 for each analysis.

Abbreviations

ADC : Arginine decarboxylase

At : *Arabidopsis thaliana*

CRE : *Cis*-acting regulatory elements

CuAO : Copper-containing amine oxidase

DILS : Dark induced leaf senescence

Hv : *Hordeum vulgare*

*Hv*PMG : *Hordeum vulgare* polyamine metabolic pathway gene

Ka : non-synonymous substitution

Ks : synonymous substitution

miRNA : Micro RNA

MYA : Million years ago

ODC : Ornithine decarboxylase

Os : *Oryza sativa*

PA : Polyamine

PAO : Polyamine oxidase

PMG : Polyamine metabolic pathway gene

PPI : Protein- protein interaction

Put : Putrescine

SAMDC : S-adenosylmethionine decarboxylase

Spd : Spermidine

SPDS : Spermidine synthase

Spm : Spermine

SPMS : Spermine synthase

TMD : Transmembrane domain

T-Spm : Thermospermine

tSPMS *:* Thermospermine synthase

Zm : *Zea mays*

Declarations

ACKNOWLEDGEMENTS

Authors are grateful to Dr. Lucyna Misztal, Department of Plant Physiology, AMU Poznan, for providing technical assistance at the initial stage of this research. Authors would like to thank Dr. Szymon Chowanski, Department of Physiology and Biology of Animal Development, AMU Poznan, for helping in the statistical data analysis. The support for Dr. Mattoo's research by the in-house ARS Project No. 8042-21000-142-00D at the United States Department of Agriculture, Beltsville, Maryland, USA, is gratefully acknowledged.

FUNDING

This research was funded by the National Science Centre, Poland (project number 2018/29/B/NZ9/00734).

AUTHORS CONTRIBUTION

UKT and ES performed the bioinformatics analysis, experimental work and analyzed the data. EPL assisted in bioinformatics analysis and conducted literature search. ESN designed and supervised the study, and interpreted the results. UKT, ES and ESN drafted the manuscript. MAJ and AKM gave suggestions on bioinformatic and experimental analysis and contributed to writing the manuscript. All authors critically revised the manuscript.

DATA AVAILABILITY

The data that support the findings of this study are available at EnsemblPlants database (https://sep2019-plants.ensembl.org/Hordeum_vulgare/Info/Index) or from the corresponding author upon reasonable request.

COMPETING INTERESTS

The authors declare no competing interests.

References

1. Monat, C., Schreiber, M., Stein, N. & Mascher, M. Prospects of pan-genomics in barley. Theor Appl Genet **132**, 785–796, doi:10.1007/s00122-018-3234-z (2019).
2. Wicker, T. *et al.* The repetitive landscape of the 5100 Mbp barley genome. Mob DNA **8**, 22, doi:10.1186/s13100-017-0102-3 (2017).
3. Munoz-Amatriain, M., Cuesta-Marcos, A., Hayes, P. M. & Muehlbauer, G. J. Barley genetic variation: implications for crop improvement. Brief Funct Genomics **13**, 341–350, doi:10.1093/bfgp/elu006 (2014).
4. Upadhyay, R. K., Fatima, T., Handa, A. K. & Mattoo, A. K. Polyamines and their biosynthesis/catabolism genes are differentially modulated in response to heat versus cold stress in tomato leaves (*Solanum lycopersicum* L.). Cells **9**, 1749 (2020).
5. Sato, S., Peet, M. & Thomas, J. Physiological factors limit fruit set of tomato (*Lycopersicon esculentum* Mill.) under chronic, mild heat stress. Plant Cell Environ **23**, 719–726 (2000).
6. Wang, X. Q., Ullah, H., Jones, A. M. & Assmann, S. M. G protein regulation of ion channels and abscisic acid signaling in Arabidopsis guard cells. Science **292**, 2070–2072, doi:10.1126/science.1059046 (2001).
7. Wang, W., Vinocur, B. & Altman, A. Plant responses to drought, salinity and extreme temperatures: towards genetic engineering for stress tolerance. Planta **218**, 1–14, doi:10.1007/s00425-003-1105-5 (2003).
8. Mittler, R. Abiotic stress, the field environment and stress combination. Trends Plant Sci **11**, 15–19, doi:10.1016/j.tplants.2005.11.002 (2006).
9. Hatfield, J. L. & Prueger, J. H. Temperature extremes: Effect on plant growth and development. Weather Clim Extrem **10**, 4–10 (2015).
10. Dresselhaus, T. & Hückelhoven, R. Biotic and abiotic stress responses in crop plants. Agronomy (Basel) **8**, 267 (2018).
11. Joshi, R., Singla-Pareek, S. L. & Pareek, A. Engineering abiotic stress response in plants for biomass production. J Biol Chem **293**, 5035–5043 (2018).
12. Waqas, M. *et al.* Genome-wide identification and expression analyses of WRKY transcription factor family members from chickpea (*Cicer arietinum* L.) reveal their role in abiotic stress-responses. Genes Genomics **41**, 467–481, doi:10.1007/s13258-018-00780-9 (2019).
13. Mattoo, A. K. Translational research in agricultural biology-enhancing crop resistivity against environmental stress alongside nutritional quality. Front Chem **2**, 30, doi:10.3389/fchem.2014.00030 (2014).
14. Tabor, C. W. & Tabor, H. Polyamines. Annu Rev Biochem **53**, 749–790, doi:10.1146/annurev.bi.53.070184.003533 (1984).
15. Mustafavi, S. H. *et al.* Polyamines and their possible mechanisms involved in plant physiological processes and elicitation of secondary metabolites. Acta Physiol Plant **40**, 102, doi:10.1007/s11738-018-2671-2 (2018).

16. Liu, W. *et al.* Functional characterization of murB-potABCD operon for polyamine uptake and peptidoglycan synthesis in *Streptococcus suis*. Microbiol Res **207**, 177–187, doi:10.1016/j.micres.2017.11.008 (2018).
17. Chen, D., Shao, Q., Yin, L., Younis, A. & Zheng, B. Polyamine Function in Plants: Metabolism, Regulation on Development, and Roles in Abiotic Stress Responses. *Front Plant Sci* **9**, 1945, doi:10.3389/fpls.2018.01945 (2018).
18. Li, M. *et al.* Genome-Wide Identification of Seven Polyamine Oxidase Genes in *Camellia sinensis* (L.) and Their Expression Patterns Under Various Abiotic Stresses. Front Plant Sci **11**, 544933, doi:10.3389/fpls.2020.544933 (2020).
19. Sobieszczuk-Nowicka, E. *et al.* Polyamines - A new metabolic switch: crosstalk with networks involving senescence, crop improvement, and mammalian cancer therapy. Front Plant Sci **10**, 859, doi:10.3389/fpls.2019.00859 (2019).
20. Kusano, T., Kim, D. W., Liu, T. & Berberich, T. in *Polyamines* 77–88 (Springer, 2015).
21. Pal, M., Szalai, G., Gondor, O. K. & Janda, T. Unfinished story of polyamines: Role of conjugation, transport and light-related regulation in the polyamine metabolism in plants. Plant Sci **308**, 110923, doi:10.1016/j.plantsci.2021.110923 (2021).
22. Miller-Fleming, L., Olin-Sandoval, V., Campbell, K. & Ralser, M. Remaining mysteries of molecular biology: The role of polyamines in the cell. J Mol Biol **427**, 3389–3406, doi:10.1016/j.jmb.2015.06.020 (2015).
23. Wang, J.-Y. & Casero, R. A. *Polyamine cell signaling: physiology, pharmacology, and cancer research*. (Springer, 2006).
24. Mehta, R. A. *et al.* Engineered polyamine accumulation in tomato enhances phytonutrient content, juice quality, and vine life. Nat Biotechnol **20**, 613–618, doi:10.1038/nbt0602-613 (2002).
25. Bányai, J. *et al.* Phenotypical and physiological study of near-isogenic durum wheat lines under contrasting water regimes. S Afr J Bot **108**, 248–255 (2017).
26. Recalde, L. *et al.* Unravelling ties in the nitrogen network: Polyamines and nitric oxide emerging as essential players in signalling roadway. Ann Appl Biol **178**, 192–208 (2021).
27. Varshney, R. K. *et al.* Translational genomics in agriculture: some examples in grain legumes. CRC Crit Rev Plant Sci **34**, 169–194 (2015).
28. Rani, A. & Kumar, V. in *Accelerated Plant Breeding, Volume 3* 343–367 (Springer, 2020).
29. Sato, K. History and future perspectives of barley genomics. DNA Res **27**, doi:10.1093/dnares/dsaa023 (2020).
30. Mascher, M. *et al.* A chromosome conformation capture ordered sequence of the barley genome. Nature **544**, 427–433, doi:10.1038/nature22043 (2017).
31. Beier, S. *et al.* Construction of a map-based reference genome sequence for barley, *Hordeum vulgare* L. Sci Data **4**, 170044, doi:10.1038/sdata.2017.44 (2017).
32. Schreiber, M. *et al.* A genome assembly of the barley 'transformation reference'cultivar Golden Promise. G3 (Bethesda) **10**, 1823–1827 (2020).
33. Planas-Portell, J., Gallart, M., Tiburcio, A. F. & Altabella, T. Copper-containing amine oxidases contribute to terminal polyamine oxidation in peroxisomes and apoplast of Arabidopsis thaliana. BMC Plant Biol **13**, 109, doi:10.1186/1471-2229-13-109 (2013).
34. Delis, C. *et al.* Ornithine decarboxylase and arginine decarboxylase gene transcripts are co-localized in developing tissues of *Glycine max* etiolated seedlings. Plant Physiol Biochem **43**, 19–25, doi:10.1016/j.plaphy.2004.11.006 (2005).
35. Ikeguchi, Y., Bewley, M. C. & Pegg, A. E. Aminopropyltransferases: function, structure and genetics. J Biochem **139**, 1–9, doi:10.1093/jb/mvj019 (2006).
36. Panicot, M. *et al.* A polyamine metabolon involving aminopropyl transferase complexes in Arabidopsis. Plant Cell **14**, 2539–2551, doi:10.1105/tpc.004077 (2002).
37. Liu, T. *et al.* Polyamine oxidase 7 is a terminal catabolism-type enzyme in *Oryza sativa* and is specifically expressed in anthers. Plant Cell Physiol **55**, 1110–1122, doi:10.1093/pcp/pcu047 (2014).
38. Ono, Y. *et al.* Constitutively and highly expressed *Oryza sativa* polyamine oxidases localize in peroxisomes and catalyze polyamine back conversion. Amino Acids **42**, 867–876, doi:10.1007/s00726-011-1002-3 (2012).
39. Hao, Y. *et al.* Identification of seven polyamine oxidase genes in tomato (*Solanum lycopersicum* L.) and their expression profiles under physiological and various stress conditions. J Plant Physiol **228**, 1–11, doi:10.1016/j.jplph.2018.05.004 (2018).
40. Ahou, A. *et al.* A plant spermine oxidase/dehydrogenase regulated by the proteasome and polyamines. J Exp Bot **65**, 1585–1603, doi:10.1093/jxb/eru016 (2014).
41. Cervelli, M. *et al.* Barley polyamine oxidase isoforms 1 and 2, a peculiar case of gene duplication. FEBS J **273**, 3990–4002, doi:10.1111/j.1742-4658.2006.05402.x (2006).
42. Rodriguez-Kessler, M. & Jimenez-Bremont, J. F. Zmspds2 maize gene: Coding a spermine synthase? Plant Signal Behav **3**, 551–553, doi:10.4161/psb.3.8.5697 (2008).
43. Trejo-Arellano, M. S. *et al.* Dark-Induced Senescence Causes Localized Changes in DNA Methylation1. Plant Physiol **182**, 949–961, doi:10.1104/pp.19.01154 (2019).
44. Distelfeld, A., Avni, R. & Fischer, A. M. Senescence, nutrient remobilization, and yield in wheat and barley. J Exp Bot **65**, 3783–3798 (2014).
45. Mückstein, U. *et al.* Thermodynamics of RNA–RNA binding. Bioinformatics **22**, 1177–1182 (2006).
46. Sobieszczuk-Nowicka, E. *et al.* Physio-genetic dissection of dark-induced leaf senescence and timing its reversal in barley. Plant Physiol **178**, 654–671 (2018).
47. Paluch-Lubawa, E., Stolarska, E. & Sobieszczuk-Nowicka, E. Dark-induced barley leaf senescence–a crop system for studying senescence and autophagy mechanisms. Front Plant Sci **12**, 425 (2021).

48. Zmienko, A. *et al.* Selection of reference genes for qPCR-and ddPCR-based analyses of gene expression in senescing barley leaves. PloS one **10**, e0118226 (2015).
49. Majumdar, R., Shao, L., Turlapati, S. A. & Minocha, S. C. Polyamines in the life of Arabidopsis: profiling the expression of S-adenosylmethionine decarboxylase (SAMDC) gene family during its life cycle. BMC Plant Biol **17**, 264, doi:10.1186/s12870-017-1208-y (2017).
50. Gong, X. *et al.* FcWRKY 70, a WRKY protein of *Fortunella crassifolia*, functions in drought tolerance and modulates putrescine synthesis by regulating arginine decarboxylase gene. Plant Cell Environ **38**, 2248–2262 (2015).
51. Tavladoraki, P., Cona, A. & Angelini, R. Copper-containing amine oxidases and FAD-dependent polyamine oxidases are key players in plant tissue differentiation and organ development. Front Plant Sci **7**, 824 (2016).
52. Wang, W., Paschalidis, K., Feng, J. C., Song, J. & Liu, J. H. Polyamine catabolism in plants: A universal process with diverse functions. Front Plant Sci **10**, 561, doi:10.3389/fpls.2019.00561 (2019).
53. Tao, Y. *et al.* The spermine synthase OsSPMS1 regulates seed germination, grain size, and yield. Plant Physiol **178**, 1522–1536 (2018).
54. Liu, T. *et al.* Genome-wide identification, phylogenetic analysis, and expression profiling of polyamine synthesis gene family members in tomato. Gene **661**, 1–10 (2018).
55. Diao, Q., Song, Y., Shi, D. & Qi, H. Interaction of polyamines, abscisic acid, nitric oxide, and hydrogen peroxide under chilling stress in tomato (*Lycopersicon esculentum* Mill.) seedlings. Front Plant Sci **8**, 203 (2017).
56. Cervelli, M. *et al.* A barley polyamine oxidase isoform with distinct structural features and subcellular localization. Eur J Biochem **268**, 3816–3830, doi:10.1046/j.1432-1327.2001.02296.x (2001).
57. Hanfrey, C., Sommer, S., Mayer, M. J., Burtin, D. & Michael, A. J. Arabidopsis polyamine biosynthesis: absence of ornithine decarboxylase and the mechanism of arginine decarboxylase activity. Plant J **27**, 551–560 (2001).
58. Galloway, G. L., Malmberg, R. L. & Price, R. A. Phylogenetic utility of the nuclear gene arginine decarboxylase: an example from Brassicaceae. Mol Biol Evol **15**, 1312–1320 (1998).
59. Gunning, P., Weinberger, R., Jeffrey, P. & Hardeman, E. Isoform sorting and the creation of intracellular compartments. Annu Rev Cell Dev Biol **14**, 339–372 (1998).
60. Bale, S. & Ealick, S. E. Structural biology of S-adenosylmethionine decarboxylase. Amino Acids **38**, 451–460, doi:10.1007/s00726-009-0404-y (2010).
61. Kim, D. W. *et al.* Polyamine oxidase 5 regulates Arabidopsis growth through thermospermine oxidase activity. Plant Physiol **165**, 1575–1590, doi:10.1104/pp.114.242610 (2014).
62. Fincato, P. *et al.* The members of Arabidopsis thaliana PAO gene family exhibit distinct tissue- and organ-specific expression pattern during seedling growth and flower development. Amino Acids **42**, 831–841, doi:10.1007/s00726-011-0999-7 (2012).
63. Fincato, P. *et al.* Functional diversity inside the Arabidopsis polyamine oxidase gene family. J Exp Bot **62**, 1155–1168, doi:10.1093/jxb/erq341 (2011).
64. Moschou, P. N. *et al.* Bridging the gap between plant and mammalian polyamine catabolism: a novel peroxisomal polyamine oxidase responsible for a full back-conversion pathway in Arabidopsis. Plant Physiol **147**, 1845–1857, doi:10.1104/pp.108.123802 (2008).
65. Cervelli, M. *et al.* A novel C-terminal sequence from barley polyamine oxidase is a vacuolar sorting signal. Plant J **40**, 410–418, doi:10.1111/j.1365-313X.2004.02221.x (2004).
66. Radova, A. *et al.* Barley polyamine oxidase: characterisation and analysis of the cofactor and the N-terminal amino acid sequence. Phytochem Anal **12**, 166–173, doi:10.1002/pca.572 (2001).
67. Sagor, G. H. M., Kusano, T. & Berberich, T. Identification of the actual coding region for polyamine oxidase 6 from rice (OsPAO6) and its partial characterization. Plant Signal Behav **12**, e1359456, doi:10.1080/15592324.2017.1359456 (2017).
68. Angelini, R. *et al.* Involvement of polyamine oxidase in wound healing. Plant Physiol **146**, 162–177, doi:10.1104/pp.107.108902 (2008).
69. Cannon, S. B., Mitra, A., Baumgarten, A., Young, N. D. & May, G. The roles of segmental and tandem gene duplication in the evolution of large gene families in Arabidopsis thaliana. BMC Plant Biol **4**, 10, doi:10.1186/1471-2229-4-10 (2004).
70. Rehman, S. *et al.* Genome wide identification and comparative analysis of the serpin gene family in brachypodium and barley. Plants (Basel) **9**, doi:10.3390/plants9111439 (2020).
71. Habachi-Houimli, Y. *et al.* Genome-wide identification, characterization, and evolutionary analysis of NBS-encoding resistance genes in barley. 3 Biotech **8**, 453, doi:10.1007/s13205-018-1478-6 (2018).
72. Andersen, E. J. *et al.* Diversity and evolution of disease resistance genes in barley (*Hordeum vulgare* L.). Evol Bioinform Online **12**, 99–108, doi:10.4137/EBO.S38085 (2016).
73. Gaut, B. S. Evolutionary dynamics of grass genomes. New Phytol **154**, 15–28 (2002).
74. Prasad, V., Stromberg, C. A., Alimohammadian, H. & Sahni, A. Dinosaur coprolites and the early evolution of grasses and grazers. Science **310**, 1177–1180, doi:10.1126/science.1118806 (2005).
75. Moore, M. J., Bell, C. D., Soltis, P. S. & Soltis, D. E. Using plastid genome-scale data to resolve enigmatic relationships among basal angiosperms. Proc Natl Acad Sci U S A **104**, 19363–19368 (2007).
76. Chaw, S. M., Chang, C. C., Chen, H. L. & Li, W. H. Dating the monocot-dicot divergence and the origin of core eudicots using whole chloroplast genomes. J Mol Evol **58**, 424–441, doi:10.1007/s00239-003-2564-9 (2004).
77. Nevo, E. in *Advance in barley sciences* 1–23 (Springer, 2013).
78. Tu, X. *et al.* Reconstructing the maize leaf regulatory network using ChIP-seq data of 104 transcription factors. Nat Commun **11**, 1–13 (2020).

79. Wallace, J. G. *et al.* Association mapping across numerous traits reveals patterns of functional variation in maize. PLoS Genet **10**, e1004845, doi:10.1371/journal.pgen.1004845 (2014).
80. Groen, S. C. *et al.* The strength and pattern of natural selection on gene expression in rice. Nature **578**, 572–576, doi:10.1038/s41586-020-1997-2 (2020).
81. Joly-Lopez, Z. *et al.* An inferred fitness consequence map of the rice genome. Nat Plants **6**, 119–130, doi:10.1038/s41477-019-0589-3 (2020).
82. Yocca, A. E. & Edger, P. P. Current status and future perspectives on the evolution of *cis*-regulatory elements in plants. Curr Opin Plant Biol **65**, 102139, doi:10.1016/j.pbi.2021.102139 (2022).
83. Porto, M. S. *et al.* Plant promoters: an approach of structure and function. Mol Biotechnol **56**, 38–49, doi:10.1007/s12033-013-9713-1 (2014).
84. Cervelli, M. *et al.* Isolation and characterization of three polyamine oxidase genes from *Zea mays*. Plant Physiol Biochem **38**, 667–677 (2000).
85. Alptekin, B., Akpinar, B. A. & Budak, H. A Comprehensive Prescription for Plant miRNA Identification. *Front Plant Sci* **7**, 2058, doi:10.3389/fpls.2016.02058 (2016).
86. Bartel, D. P. MicroRNAs: genomics, biogenesis, mechanism, and function. Cell **116**, 281–297, doi:10.1016/s0092-8674(04)00045-5 (2004).
87. Rhoades, M. W. *et al.* Prediction of plant microRNA targets. Cell **110**, 513–520, doi:10.1016/s0092-8674(02)00863-2 (2002).
88. Dang, T. H. Y., Ziemann, M. & Bhave, M. in *Barley: physical properties, genetic factors and environmental impacts on growth.* (ed Kohji Hasunuma) 165–192 (Nova Science Publishers, 2014).
89. Kumar, R. Role of microRNAs in biotic and abiotic stress responses in crop plants. Appl Biochem Biotechnol **174**, 93–115, doi:10.1007/s12010-014-0914-2 (2014).
90. Sunkar, R., Li, Y. F. & Jagadeeswaran, G. Functions of microRNAs in plant stress responses. Trends Plant Sci **17**, 196–203, doi:10.1016/j.tplants.2012.01.010 (2012).
91. Kantar, M., Unver, T. & Budak, H. Regulation of barley miRNAs upon dehydration stress correlated with target gene expression. Funct Integr Genomics **10**, 493–507, doi:10.1007/s10142-010-0181-4 (2010).
92. Hackenberg, M., Shi, B. J., Gustafson, P. & Langridge, P. A transgenic transcription factor (TaDREB3) in barley affects the expression of microRNAs and other small non-coding RNAs. PLoS One **7**, e42030, doi:10.1371/journal.pone.0042030 (2012).
93. Wu, L. *et al.* Identification of microRNAs in response to aluminum stress in the roots of Tibetan wild barley and cultivated barley. BMC Genomics **19**, 560, doi:10.1186/s12864-018-4953-x (2018).
94. Hackenberg, M., Gustafson, P., Langridge, P. & Shi, B. J. Differential expression of microRNAs and other small RNAs in barley between water and drought conditions. Plant Biotechnol J **13**, 2–13, doi:10.1111/pbi.12220 (2015).
95. Liu, B. & Sun, G. MicroRNAs contribute to enhanced salt adaptation of the autopolyploid *Hordeum bulbosum* compared with its diploid ancestor. Plant J **91**, 57–69 (2017).
96. Inal, B. *et al.* Genome-wide fungal stress responsive miRNA expression in wheat. Planta **240**, 1287–1298, doi:10.1007/s00425-014-2153-8 (2014).
97. Zhao, J., Missihoun, T. D. & Bartels, D. The role of Arabidopsis aldehyde dehydrogenase genes in response to high temperature and stress combinations. J Exp Bot **68**, 4295–4308, doi:10.1093/jxb/erx194 (2017).
98. Guo, J. *et al.* Aldehyde dehydrogenase plays crucial roles in response to lower temperature stress in *Solanum tuberosum* and *Nicotiana benthamiana*. Plant Sci **297**, 110525, doi:10.1016/j.plantsci.2020.110525 (2020).
99. Wang, W. *et al.* Genome-wide characterization of the aldehyde dehydrogenase gene superfamily in soybean and its potential role in drought stress response. BMC Genomics **18**, 518, doi:10.1186/s12864-017-3908-y (2017).
100. Tola, A. J., Jaballi, A., Germain, H. & Missihoun, T. D. Recent development on plant aldehyde dehydrogenase enzymes and their functions in plant development and stress signaling. Genes **12**, 51 (2021).
101. Fabiano, C., Tezotto, T., Favarin, J. L., Polacco, J. C. & Mazzafera, P. Essentiality of nickel in plants: a role in plant stresses. Front Plant Sci **6**, 754 (2015).
102. Rangan, P., Subramani, R., Kumar, R., Singh, A. K. & Singh, R. Recent advances in polyamine metabolism and abiotic stress tolerance. *Biomed Res Int* 2014, 239621, doi:10.1155/2014/239621 (2014).
103. Alcazar, R. *et al.* Polyamines: molecules with regulatory functions in plant abiotic stress tolerance. Planta **231**, 1237–1249, doi:10.1007/s00425-010-1130-0 (2010).
104. Sobieszczuk-Nowicka, E. Polyamine catabolism adds fuel to leaf senescence. Amino Acids **49**, 49–56, doi:10.1007/s00726-016-2377-y (2017).
105. Sequera-Mutiozabal, M. I. *et al.* Global metabolic profiling of Arabidopsis polyamine oxidase 4 (AtPAO4) loss-of-function mutants exhibiting delayed dark-induced senescence. Front Plant Sci **7**, 173 (2016).
106. Sobieszczuk-Nowicka, E., Kubala, S., Zmienko, A., Małecka, A. & Legocka, J. From accumulation to degradation: reprogramming polyamine metabolism facilitates dark-induced senescence in barley leaf cells. Front Plant Sci **6**, 1198 (2016).
107. Bartlett, J. G., Alves, S. C., Smedley, M., Snape, J. W. & Harwood, W. A. High-throughput Agrobacterium-mediated barley transformation. Plant Methods **4**, 1–12 (2008).
108. Smedley, M. A. & Harwood, W. A. in *Agrobacterium Protocols* (ed Wang K.) 3–16 (Springer, 2015).
109. Holme, I. B. *et al.* Evaluation of the mature grain phytase candidate HvPAPhy_a gene in barley (*Hordeum vulgare* L.) using CRISPR/Cas9 and TALENs. Plant Mol Biol **95**, 111–121 (2017).
110. Upadhyay, R. K. & Mattoo, A. K. Genome-wide identification of tomato (*Solanum lycopersicum* L.) lipoxygenases coupled with expression profiles during plant development and in response to methyl-jasmonate and wounding. J Plant Physiol **231**, 318–328, doi:10.1016/j.jplph.2018.10.001 (2018).

111. Finn, R. D., Clements, J. & Eddy, S. R. HMMER web server: interactive sequence similarity searching. Nucleic Acids Res **39**, W29-37, doi:10.1093/nar/gkr367 (2011).
112. Finn, R. D. *et al.* InterPro in 2017-beyond protein family and domain annotations. Nucleic Acids Res **45**, D190-D199, doi:10.1093/nar/gkw1107 (2017).
113. Procter, J. B. *et al.* Alignment of Biological Sequences with Jalview. Methods Mol Biol **2231**, 203–224, doi:10.1007/978-1-0716-1036-7_13 (2021).
114. Drozdetskiy, A., Cole, C., Procter, J. & Barton, G. J. JPred4: a protein secondary structure prediction server. Nucleic Acids Res **43**, W389-394, doi:10.1093/nar/gkv332 (2015).
115. Tamura, K., Stecher, G. & Kumar, S. MEGA11: Molecular Evolutionary Genetics Analysis Version 11. Mol Biol Evol **38**, 3022–3027, doi:10.1093/molbev/msab120 (2021).
116. Chen, C., Chen, H., He, Y. & Xia, R. TBtools, a toolkit for biologists integrating various biological data handling tools with a user-friendly interface. BioRxiv **289660**, 289660 (2018).
117. Wang, Y. *et al.* MCScanX: a toolkit for detection and evolutionary analysis of gene synteny and collinearity. Nucleic Acids Res **40**, e49, doi:10.1093/nar/gkr1293 (2012).
118. Lynch, M. & Conery, J. S. The evolutionary fate and consequences of duplicate genes. Science **290**, 1151–1155, doi:10.1126/science.290.5494.1151 (2000).
119. Cui, L., Yang, G., Yan, J., Pan, Y. & Nie, X. Genome-wide identification, expression profiles and regulatory network of MAPK cascade gene family in barley. BMC Genomics **20**, 750, doi:10.1186/s12864-019-6144-9 (2019).
120. Ju, L. *et al.* Structural organization and functional divergence of high isoelectric point alpha-amylase genes in bread wheat (*Triticum aestivum* L.) and barley (*Hordeum vulgare* L.). BMC Genet **20**, 25, doi:10.1186/s12863-019-0732-1 (2019).
121. Wolfe, K. H., Sharp, P. M. & Li, W.-H. Rates of synonymous substitution in plant nuclear genes. J Mol Evol **29**, 208–211 (1989).
122. Rombauts, S., Dehais, P., Van Montagu, M. & Rouze, P. PlantCARE, a plant *cis*-acting regulatory element database. Nucleic Acids Res **27**, 295–296, doi:10.1093/nar/27.1.295 (1999).
123. Dai, X., Zhuang, Z. & Zhao, P. X. psRNATarget: a plant small RNA target analysis server (2017 release). Nucleic Acids Res **46**, W49-W54, doi:10.1093/nar/gky316 (2018).
124. Szklarczyk, D. *et al.* The STRING database in 2021: customizable protein-protein networks, and functional characterization of user-uploaded gene/measurement sets. Nucleic Acids Res **49**, D605-D612, doi:10.1093/nar/gkaa1074 (2021).
125. Papatheodorou, I. *et al.* Expression Atlas update: from tissues to single cells. Nucleic Acids Res **48**, D77-D83, doi:10.1093/nar/gkz947 (2020).
126. Hruz, T. *et al.* Genevestigator v3: a reference expression database for the meta-analysis of transcriptomes. *Adv Bioinformatics* 2008, 420747, doi:10.1155/2008/420747 (2008).
127. Grennan, A. K. Genevestigator. Facilitating web-based gene-expression analysis. Plant Physiol **141**, 1164–1166 (2006).
128. Pfaffl, M. W. A new mathematical model for relative quantification in real-time RT-PCR. *Nucleic Acids Res* **29**, e45, doi:10.1093/nar/29.9.e45 (2001).

Figures

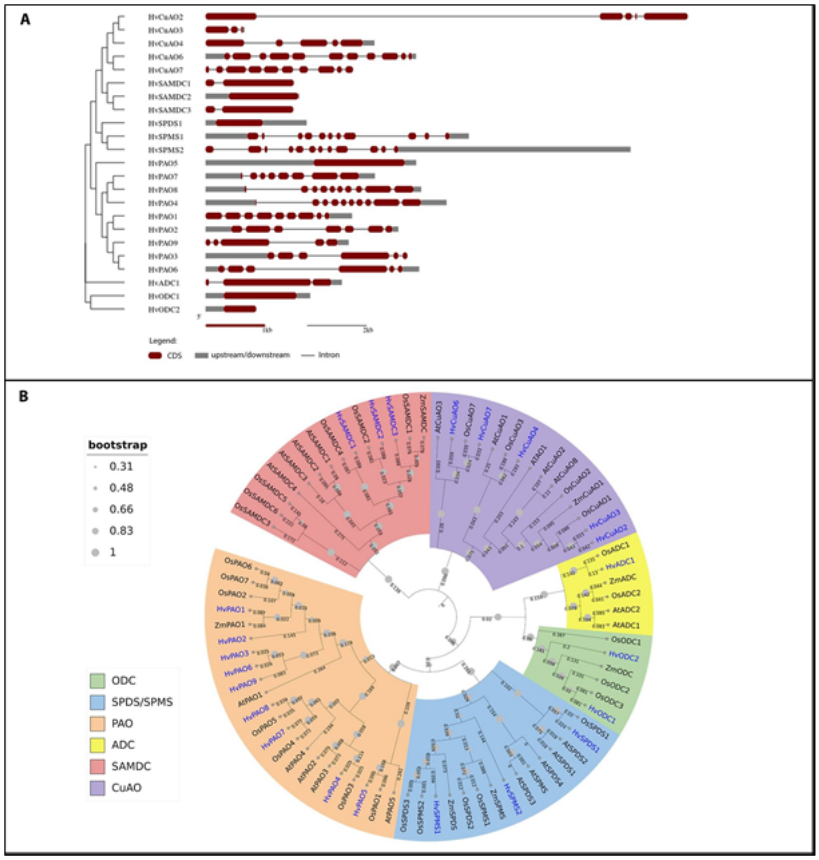

Figure 1

Gene structure and phylogenetic relationship of polyamine metabolic pathway genes in barley. (A) Gene structure; (B) Comparative phylogenetic relationships of polyamine metabolic pathway proteins in barley (*Hv*), Arabidopsis (*At*), rice (*Os*) and maize (*Zm*) plants. The tree was constructed using neighbor-joining method with 1000 bootstrap replications in MEGA-11. The barley genes identified in the present study are hilighted in blue color. The accession numbers of the genes used in this analysis are presented in Supplementary Table S1. *ADC* (arginine decarboxylase); *SAMDC* (S-adenosylmethionine decarboxylase); *SPDS* (spermidine synthase); *SPMS* (spermine synthase); *CuAO* (Diamine or copper-containing oxidase); and *PAO* (polyamine oxidase) in barley (*Hv*).

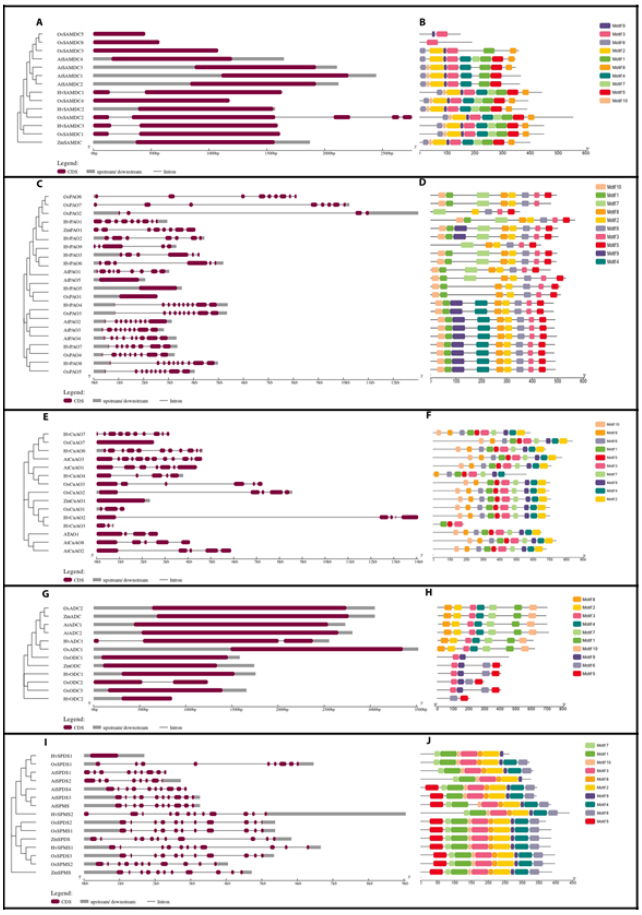

Figure 2

Gene structure and protein motif constructions of polyamine metabolic genes in plants, barley (*Hv*), Arabidopsis (*At*), rice (*Os*) and maize (*Zm*). (A, B) S-adenosylmethionine decarboxylase; (C, D) polyamine oxidase; (E, F) copper-containing amine oxidase; (G, H) arginine decarboxylase and ornithine decarboxylase; (I, J) spermidine/spermine synthase. *ADC* (arginine decarboxylase); *SAMDC* (S-adenosylmethionine decarboxylase); *SPDS* (spermidine synthase); *SPMS* (spermine synthase); CuAO (Diamine or copper-containing oxidase); and *PAO* (polyamine oxidase) in barley (*Hv*).

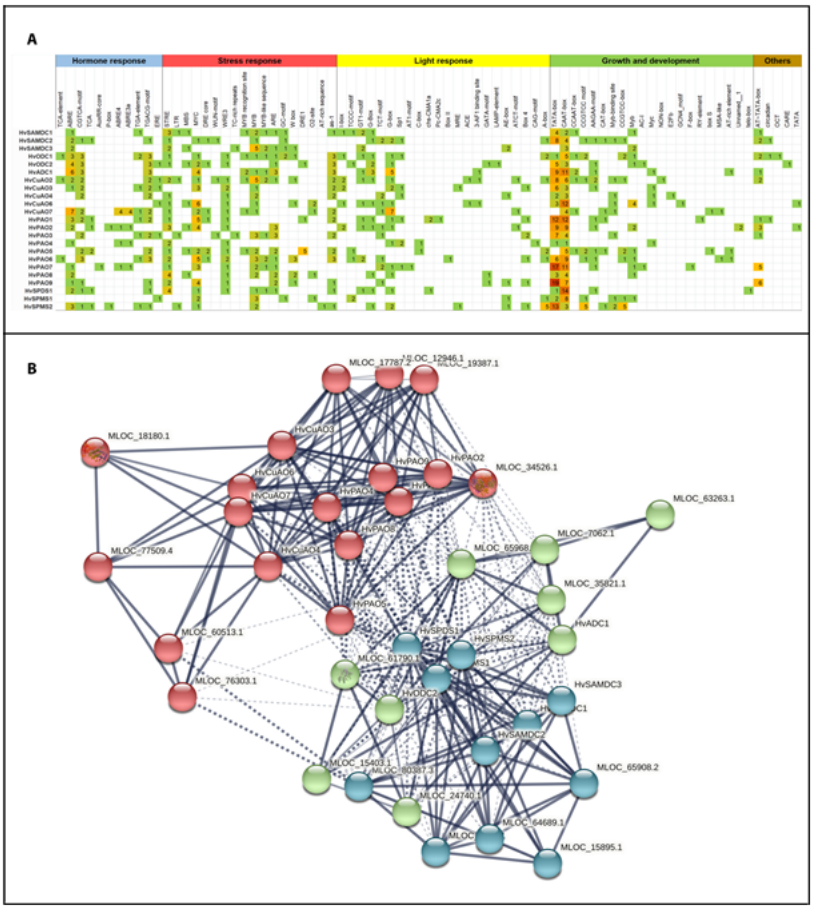

Figure 3

(A) Distribution of putative *cis*-acting regulatory elements in 1000 bp upstream regions of polyamine metabolic pathway genes; and (B) protein interaction network of polyamine metabolic pathway proteins in barley. The nodes (circles) represent proteins while the straight lines represent the interactions between different proteins. Nodes in red colour denote Cluster 1, in green colour Cluster 2 and in blue colour Cluster 3. *ADC* (arginine decarboxylase); *SAMDC* (S-adenosylmethionine decarboxylase); *SPDS* (spermidine synthase); *SPMS* (spermine synthase); CuAO (Diamine or copper-containing oxidase); and *PAO* (polyamine oxidase) in barley (*Hv*).

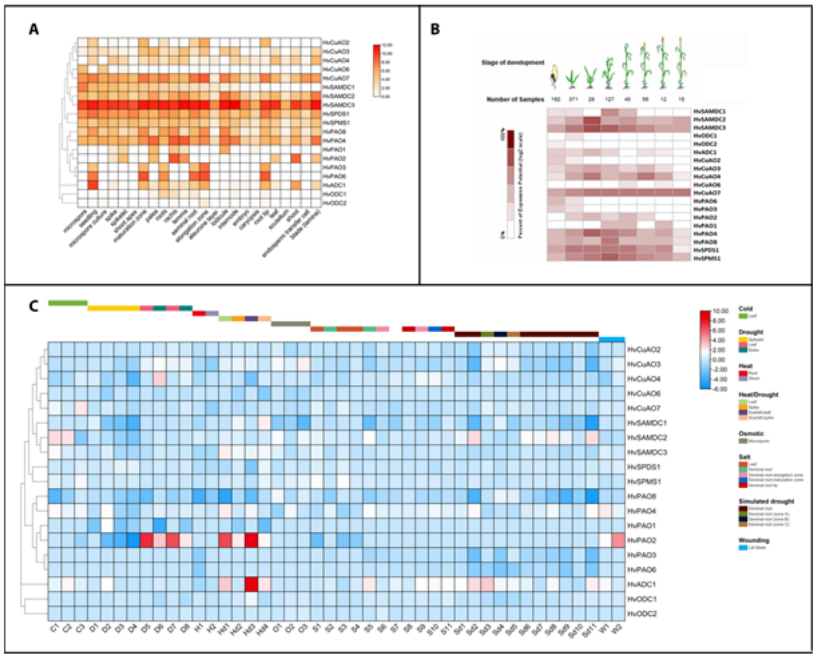

Figure 4

Expression patterns of barley polyamine metabolic pathway genes. (A) In different tissues; (B) during the developmental growth stages; and (C) barley during different stress conditions. C1: cold (-2°C; 4h)/untreated leaf samples (4h), C2: cold (-8°C;18h)/untreated leaf samples (18h), C3: cold (3/1°C; 5d)/untreated leaf samples (5d), D1: drought (B1K0412)/untreated spikelet samples (B1K0412), D2: drought (B1K3516)/untreated spikelet samples (B1K3516), D3: drought (B1K3615)/untreated spikelet samples (B1K3615), D4: drought (B1K4620)/untreated spikelet samples (B1K4620), D5: drought (SBCC073; leaf)/untreated leaf samples (SBCC073), D6: drought (SBCC073; spike)/untreated spike samples (SBCC073), D7: drought (Scarlett; leaf)/untreated leaf samples (Scarlett), D8: drought (Scarlett; spike)/untreated spike samples (Scarlett), H1: heat (root)/untreated root samples, H2: heat (shoot)/untreated shoot samples, Hd1: heat; drought (SBCC073; leaf)/untreated leaf samples (SBCC073), Hd2: heat; drought (SBCC073; spike)/untreated spike samples (SBCC073), Hd3: heat; drought (Scarlett; leaf)/untreated leaf samples (Scarlett), Hd4: heat; drought (Scarlett; spike)/untreated spike samples (Scarlett), O1: osmotic; 26°C/untreated microspore samples, O2: osmotic; 26°C; microspore culture/osmotic; 26°C, O3: osmotic; 26°C; microspore culture/ untreated microspore samples, S1: salt (2h)/untreated leaf samples, S2: salt (6h)/untreated seminal root samples (6h), S3: salt (12h)/untreated leaf samples, S4: salt (24h)/untreated leaf samples, S5: salt (24h)/untreated seminal root samples (24h), S6: salt (Clipper; elongation zone)/untreated seminal root elongation zone samples (Clipper), S7: salt (Clipper; maturation zone)/untreated seminal root maturation zone samples (Clipper), S8: salt (Clipper; root tip)/untreated seminal root tip samples (Clipper), S9: salt (Sahara 3771; elongation zone)/untreated seminal root elongation zone samples (Sahara 3771), S10: salt (Sahara 3771; maturation zone)/untreated seminal root maturation zone samples (Sahara 3771), S11: salt (Sahara 3771; root tip)/untreated seminal root tip samples (Sahara 3771), Sd1: simulated drought (6h)/untreated seminal root samples (6h), Sd2: simulated drought (24h)/untreated seminal root samples (24h), Sd3: simulated drought (zone A)/untreated seminal root samples (zone A), Sd4: simulated drought (zone B)/untreated seminal root samples (zone B), Sd5: simulated drought (zone C)/untreated seminal root samples (zone C), Sd6: simulated drought, salt (6h)/salt (6h), Sd7: simulated drought, salt (6h)/simulated drought (6h), Sd8: simulated drought, salt (6h)/untreated seminal root samples (6h), Sd9: simulated drought, salt (24h)/salt (24h), Sd10: simulated drought, salt (24h)/simulated drought (24h), Sd11: simulated drought, salt (24h)/untreated seminal root samples (24h), W1: wounding (2h)/untreated leaf blade samples, and W2: wounding (24h)/untreated leaf blade samples. All the data were curated from the mRNA-Seq Gene Level *Hordeum vulgare* (ref: Morex V3) and Affymetrix Barley Genome Array databases on GENEVESTIGATOR. *ADC* (arginine decarboxylase); *SAMDC* (S-adenosylmethionine decarboxylase); *SPDS* (spermidine synthase); *SPMS* (spermine synthase); CuAO (Diamine or copper-containing oxidase); and *PAO* (polyamine oxidase) in barley (*Hv*).

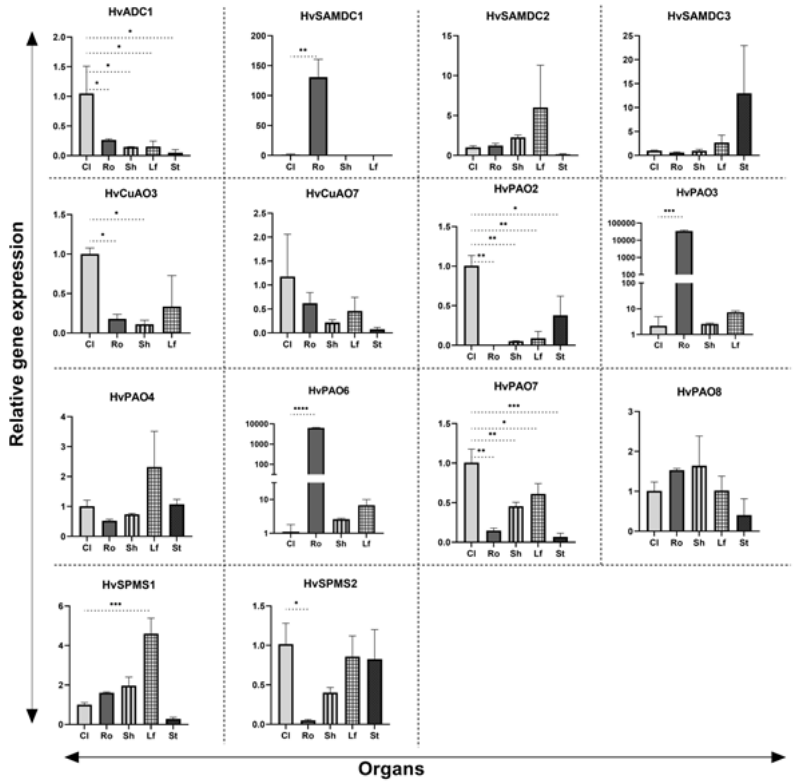

Figure 5

Expression levels of polyamine metabolic pathway genes in Cl, coleoptile; Ro, root; Sh, shoot; Lf, leaf; St, stem of barley. Relative expression in the coleoptile was assumed as 1.0 using *H. vulgare* actin gene (AY145451) as the reference gene. Data represent mean values and standard deviation of at least two biological replicates with three technical repetitions. ANOVA with Dunnett's multiple comparisons test was performed for significant differences. Statistical significance between data points was assessed against coleoptile (Cl) versus expression profiles of other organs and categorized as *P<0.05, **P<0.01, ***P<0.001 and ****P<0.0001using Graph pad (version 9.3.1). *ADC* (arginine decarboxylase); *SAMDC* (S-adenosylmethionine decarboxylase); *SPDS* (spermidine synthase); *SPMS* (spermine synthase); CuAO (Diamine or copper-containing oxidase); and *PAO* (polyamine oxidase) in barley (*Hv*).

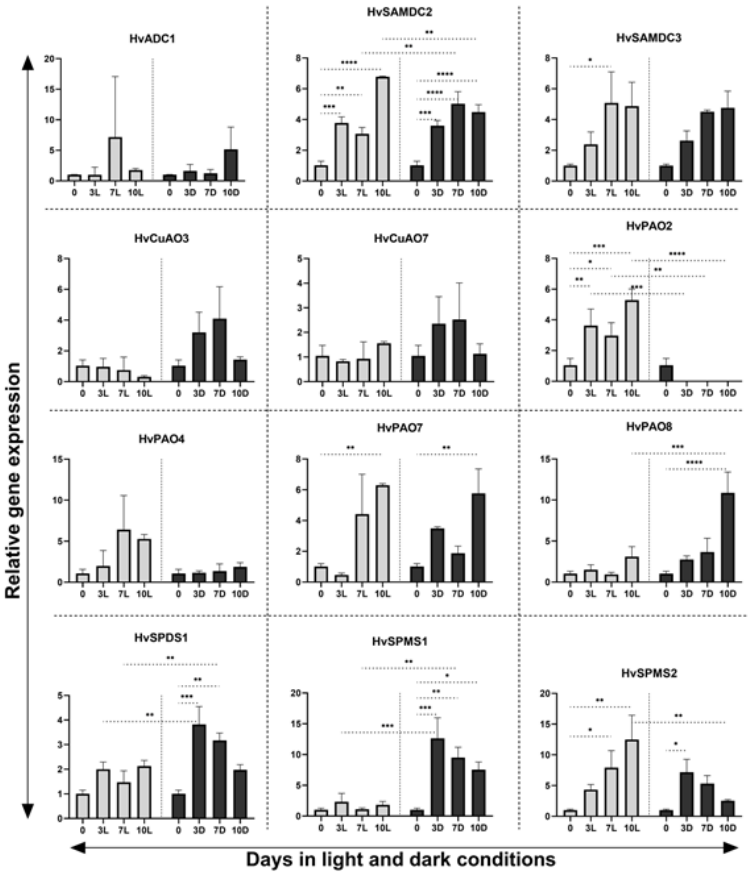

Figure 6

Comparative qRT-PCR analysis of polyamine metabolic pathway genes in barley during dark induced leaf senescence. 0, day-0; 3L, day-3 in light; 7L, day-7 in light; 10L, day-10 in light; 3D, day-3 in dark; 7D, day-7 in dark; 10D, day-10 in dark. Relative expression on day-0 was assumed as 1.0 using *H. vulgare* pyruvate kinase family protein gene (AK356185) as the reference gene [48]. The experiment included three biological and three technical replicates. ANOVA with Bonferroni's multiple comparisons test was performed for significant differences. Statistical significance between data points was assessed against day-0 (control) timepoints versus other timepoints of expression profiles (day-3, 7 and 10) and each timepoint in light and dark, and were categorized as *P<0.05, **P<0.01, ***P<0.001 and ****P<0.0001 using Graph pad (version 9.3.1). *ADC* (arginine decarboxylase); *SAMDC* (S-adenosylmethionine decarboxylase); *SPDS* (spermidine synthase); *SPMS* (spermine synthase); CuAO (Diamine or copper-containing oxidase); and *PAO* (polyamine oxidase) in barley (*Hv*).

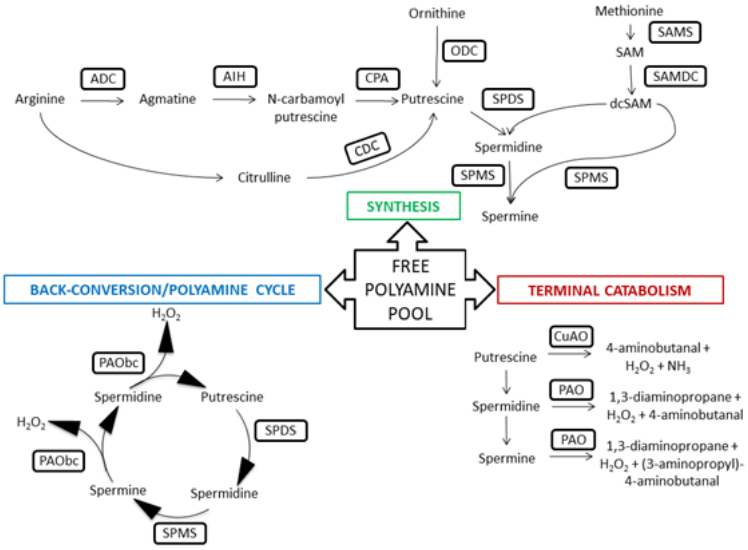

Figure 7

Polyamine (PAs) metabolic pathway genes involved in the formation of the free PAs pool in plant cells. PAs synthesis in plants involves the independent decarboxylation of two amino acids, ornithine and arginine. Decarboxylation of arginine by arginine decarboxylase (*ADC*) yields agmatine, which is then hydrolyzed to putrescine. In contrast, the decarboxylation of ornithine by ornithine decarboxylase (*ODC*) directly produces putrescine. Subsequent decarboxylation of S-adenosylmethionine (SAM) catalyzed by S-adenosylmethionine decarboxylase (*SAMDC*) produces decarboxylated SAM as the source of propylamine groups, which in turn complex with putrescine to produce spermidine catalyzed by spermidine synthase (*SPDS*). Spermidine and another molecule of decarboxylated SAM become substrates for spermine synthase (*SPMS*) to produce spermine. Diamine or copper-containing oxidase (*CuAO*) and polyamine oxidase (*PAO*) catalyze the deamination of polyamines. In some tissues, the back-conversion pathway is prevalent. It involves oxidation of spermine to spermidine, which is then oxidized to putrescine catalyzed by polyamine oxidase (*PAObc*) Abbreviations: AIH, agmatine iminohydrolase; CDC, citrulline decarboxylase; CPA, N-carbamoyl putrescine amidohydrolase; modified from Pál et al., [21].

Supplementary Files

This is a list of supplementary files associated with this preprint. Click to download.

- SupplementaryFigures.docx
- SupplementaryTables.docx